NASA TECHNICAL NOTE

NASA TN D-4243

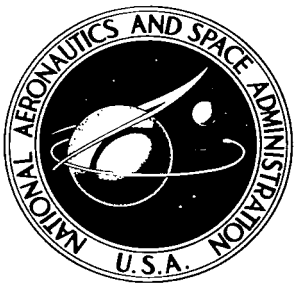

C.1

TECH LIBRARY KAFB, NM
0130838

LOAN COPY: RETURN TO
AFWL (WLIL-2)
KIRTLAND AFB, N MEX

NASA TN D-4243

AN EVALUATION OF THE THERMALLY RADIANT ENVIRONS OF A MAN ON THE LUNAR SURFACE

by David H. Perel and Alan J. Chapman

Manned Spacecraft Center
Houston, Texas

NATIONAL AERONAUTICS AND SPACE ADMINISTRATION • WASHINGTON, D. C. • NOVEMBER 1967

TECH LIBRARY KAFB, NM
0130838
NASA TN D-4243

AN EVALUATION OF THE THERMALLY RADIANT ENVIRONS OF A MAN ON THE LUNAR SURFACE

By David H. Perel and Alan J. Chapman

Manned Spacecraft Center
Houston, Texas

NATIONAL AERONAUTICS AND SPACE ADMINISTRATION

For sale by the Clearinghouse for Federal Scientific and Technical Information
Springfield, Virginia 22151 – CFSTI price $3.00

ABSTRACT

A method was established for evaluating the effects of radiative heat energy incident upon a man on the lunar surface. The results were used to plot the topography of a plain over a wide range of variables to allow solutions for many specific conditions. Radiation from both illuminated and dark areas was evaluated.

CONTENTS

FIGURES

AN EVALUATION OF THE THERMALLY RADIANT ENVIRONS OF A MAN ON THE LUNAR SURFACE

By David H. Perel and Alan J. Chapman
Manned Spacecraft Center

SUMMARY

Analytical methods were developed for determining the quantities of radiative thermal energy to provide a quantitative evaluation of the effects of the lunar thermal environment on a pressure-suited man. Evaluations were limited to lunar plains. A multicylinder man and a hemisphere-cylinder man were considered in the analysis. While emphasis was placed on the evaluation of quantities of thermal radiation from the lighted side of the moon, the radiation on the dark portion was also considered and illustrated. The results of the investigation are presented in parametric form to allow the solution of specific problems over a wide range of variables.

INTRODUCTION

One of the environmental factors to be considered before a pressure-suited man can be landed on the moon is the effect of the thermal radiation which will be incident upon him. Evaluations of this thermal radiation are limited herein to the lunar plain. A simplified version of the familiar technique for the determination of radiant energy exchange is applied to the analysis of the amounts of thermal radiation incident upon the man.

SYMBOLS

A, A_1 areas of two finite surfaces, ft^2

A_p projected area, ft^2

A_{p_s} projected area of hemisphere-cylinder man, normal to sun's rays, ft^2

A_t total surface area, ft^2

a	semimajor diameter of the ellipse, moon's albedo, ft
b	semiminor diameter of the ellipse, ft
C	distance from the plain to the midpoint of the cylinder, ft
C_p	projected circumference of the ellipse, ft
D	diameter of the cylinder, ft
e	lunar emissive power, Btu/hr-ft^2
F	geometric shape factor of man with respect to the lunar surface
F_{A-A_1}	geometric shape factor of A with respect to area A_1
F_m	ratio of the projected surface area of the man, normal to the sun's rays, to the total surface
F_s	G_n/G_s
G_n	solar flux normal to the lunar surface, Btu/hr-ft^2
G_s	normal flux at the subsolar point, Btu/hr-ft^2
H	height of the cylinder, ft
J	surface radiosity, Btu/hr-ft^2
k	thermal conductivity of pressure suit, Btu/hr-ft-°F
q	thermal energy, Btu/hr-ft^2
q_{abs}	total radiant heat absorbed by the man, Btu/hr-ft^2
q_{am}	radiation absorbed from the moon's albedo, Btu/hr-ft^2
q_c	heat conducted through the insulation, Btu/hr-ft^2
q_{em}	radiation absorbed from the moon's emittance, Btu/hr-ft^2
q_r	heat radiated by the surface, Btu/hr-ft^2

q_s radiation absorbed from direct solar radiation, Btu/hr-ft^2

R finite radius, ft

r plane radius, ft

T surface temperature, °R

T_i temperature of inner skin of the insulation, °F

U $k/\Delta x$, conductance, Btu/hr-ft^2-°F

x, y, z spatial coordinates

α_s solar absorptivity

β angle made by normal and radius from plane to point on surrounding hemisphere, deg

γ angle made by normal to plane and line from emitting surface to receiving surface, deg

Δx thickness of insulating material, ft

ϵ emissivity

θ plane angle, deg

$\theta_{q_{max}}$ angle of maximum absorption, deg

ρ distance of emitting surface from receiving surface, ft

σ Stefan-Boltzmann constant, Btu/hr-ft^2-°R^4

ϕ angle between normal to emitting surface and line of sight to cylinder, deg

Ψ angle defined in figure A-1, deg

ω angle between plane and line of sight of cliff to cylinder, deg

THERMAL RADIATION CONCEPTS

Figure 1 depicts the terminology involved. Two finite surfaces, A and A_1, are oriented arbitrarily in space. The amount of direct thermal radiation received by A

because of energy leaving A_1, per unit of receiving surface area (ref. 1), is given by the equation

$$\frac{q}{A} = F_{A\text{-}A_1} J_{A_1} \tag{1}$$

where $F_{A\text{-}A_1}$ is the geometric shape factor of A_1 with respect to A and J_{A_1} is the radiosity of surface A_1, including original emission and radiation reflected from external sources. The shape factor, in terms of the nomenclature of figure 1, is defined by the equation

$$F_{A\text{-}A_1} = \frac{1}{A} \int_A \int_{A_1} \frac{\cos \beta \cos \gamma \, dA \, dA}{\pi \rho^2} \tag{2}$$

The previous expression for $F_{A\text{-}A_1}$ assumes that the surface radiosity (both emission and reflection) is diffuse and follows Lambert's law. While this assumption is not strictly true for the lunar surface, it will be considered adequate for the purposes of this paper.

The heat flux incident upon the receiving surface q/A, given in equations (1) and (2), includes only the direct exchange from A_1 to A; no multiple reflections between the two surfaces are considered. Successful use of equation (2) requires the formulation of dA_1 and dA (the area elements), ρ (the distance between the area elements), and $\cos \beta$ and $\cos \gamma$ (the angles between the surface normals and ρ) in terms of conveniently selected coordinates. The subsequent integrations must then be carried out. Except for the simplest geometries, the preceding procedures usually become quite complex. For the purpose of the present analysis, a simplified, approximate approach may be adopted.

If the surface A_1 is taken to represent the lunar surface, it may be considered to be a plane of infinite extent. With this consideration, a simplification of equation (2) may be made without incurring serious error. If A (the receiving surface) is small compared to A_1 (the emitting surface) and if ρ (the separation distance) is large, ρ and β may be assumed to change very little as the integration over A is performed. Then

$$F_{A\text{-}A_1} \approx \frac{1}{A} \int_{A_1} \frac{\cos \beta}{\pi \rho^2} \left[\int_A \cos \gamma \, dA \right] dA \tag{3}$$

The integral $\int_A \cos \gamma \, dA$ is the projected view of the surface A as seen from the emitting element dA_1. Using A_p to denote this projection,

$$F_{A-A_1} \approx \frac{1}{A} \int_{A_1} \frac{\cos \beta \, A_p}{\pi \rho^2} \, dA \tag{4}$$

This simplified formulation amounts to the presumption that all rays between A and dA_1 are essentially parallel. Usually A_p may be conveniently expressed in terms of the position of dA_1 by further use of the parallel-ray assumption. Likewise, the angle β and the distance ρ may be measured with respect to some suitable midpoint of the projected area A_p (ref. 2).

HEAT RADIATION FROM A LUNAR PLAIN

Effects on a Multicylinder Man

A possible representation of a man on the lunar surface is that of a combination of cylinders: the head, the arms, and the legs are right circular cylinders, and the torso is an elliptical cylinder. The arrangements and the dimensions of these cylinders are shown in figure 2. These dimensions were taken from the recommendations of reference 3. The method outlined in the previous section will now be applied to the determination of the fraction of the energy leaving each element of the multicylinder man which strikes the lunar surface. A value for the entire multicylinder man may then be found.

Head. - Figure 3 shows the geometry of the cylinder representative of the head. To use equations (1) and (4) to determine the quantity of thermal energy which radiates from the lunar plain and strikes the head, the projected area of the head as viewed from a point on the plain must be defined. The line of sight is taken from dA_1 to the midpoint of the cylinder. Along the line of sight, the projected area of the cylinder is a complex curvilinear trapezoid. However, in accordance with the parallel-ray assumption previously noted, this projected area is taken as a rectangle so that $A_p = HD \sin \phi$, where H and D are the height and the diameter, respectively, of the cylinder. The shape factor of the head with respect to a circular plane of finite radius R is

$$F_{head} = \frac{4HD}{HD\pi} \int_{\theta=0}^{\pi/2} \int_{r=0}^{r=R} \frac{\cos \phi \, \sin \phi \, r \, dr \, d\theta}{\pi \rho^2} \tag{5}$$

where ϕ is the angle between the normal to dA and the line of sight to the cylinder, ρ is the distance from dA to the man, and r is the distance of dA from the vertical axis of the cylinder.

In equation (5), $\sin\phi$, $\cos\phi$, and ρ may be expressed in terms of r and the distance from the plain to the midpoint of the cylinder C. Subsequent integration yields

$$F_{head} = \frac{1}{\pi}\left[\tan^{-1}\left(\frac{R}{C}\right) - \frac{\left(\frac{R}{C}\right)}{\left(\frac{R}{C}\right)^2 + 1}\right] \tag{6}$$

For a realistic value of C = 5.5 feet, evaluation of equation (6) for various values of the radius R gives

R, ft	50	100	500	1000	10 000
F_{head}	0.431	0.465	0.493	0.496	0.4999

When the lunar surface is taken as infinite ($R \to \infty$), the distance C is eliminated as a significant variable and equation (6) yields

$$F_{head} = 0.5 \tag{7}$$

a fact which is readily predicted by basic reasoning. For a height of 5.5 feet, the lunar horizon is more than 2 miles distant, and the preceding calculations reveal that the representation of the lunar surface as an infinite disk is a reasonable assumption for these purposes.

Torso. - The torso, an elliptical cylinder, is considered in figure 4. The shape factor is found by taking the projected area to be a rectangle so that $A_p = HC_p \sin\phi$, where C_p represents the width of the ellipse as viewed from dA_1. Thus, as a result of a parallel-ray assumption, C_p is a function of the angle θ. If a and b represent, respectively, the semimajor and semiminor diameters of the ellipse, the derivation in appendix A shows

$$C_p = 2a\sqrt{1 - \frac{a^2 - b^2}{a^2}\cos^2\theta} \tag{8}$$

The projected area A_p, viewed from a point on the lunar plain, is then

$$A_p = C_p H \sin \phi$$

so that the shape factor with respect to a circular disk of radius R becomes

$$F_{torso} = \frac{4H}{A_{torso}} \int_{\theta=0}^{\pi/2} \int_{r=0}^{R} \frac{\cos \phi \sin \phi \, C_p r \, dr \, d\theta}{\pi \rho^2}$$

$$= \frac{2H}{\pi} \left[\tan^{-1}\left(\frac{R}{C}\right) - \frac{\left(\frac{R}{C}\right)}{\left(\frac{R}{C}\right)^2 + 1} \right] \frac{1}{A_{torso}} \int_0^{\pi/2} C_p \, d\theta \tag{9}$$

For an elliptic cylinder

$$A_{torso} = 4Ha \int_0^{\pi/2} \sqrt{1 - \left(\frac{a^2 - b^2}{a^2}\right) \sin \theta} \, d\theta \tag{10}$$

When equation (10) and equation (8) are combined with equation (9), the results are

$$F_{torso} = \frac{1}{\pi} \left[\tan^{-1}\left(\frac{R}{C}\right) - \frac{\left(\frac{R}{C}\right)}{\left(\frac{R}{C}\right)^2 + 1} \right] = F_{head} \tag{11}$$

Thus, within the parallel-ray representation of the shape factor, the same result is obtained for the circular cylinder and the elliptic cylinder. Likewise, as $R \to \infty$

$$F_{torso} = 0.5 \tag{12}$$

Arm. - The arm is represented by a right circular cylinder the axis of which is parallel to the surface of the plain. Any shielding, by or of the body, is neglected. Using the nomenclature of figure 5 and applying equation (4) gives

$$F_{arm} = \frac{4HD}{\pi HD} \int_{\sigma=0} \int_{r=0} \frac{C\left(C^2 + r^2\cos^2\sigma\right)^{1/2} r\, dr\, d\sigma}{\pi\left(r^2 + C^2\right)^2} \tag{13}$$

Rather than integrate the above expression, and since later application of this analysis will be made in instances in which the lunar surface is taken as an infinite plane, the following result as $R \to \infty$ is obtained by simple physical reasoning

$$F_{arm} = 0.5 \tag{14}$$

Legs. - The heat flux incident between the legs and the lunar surface is considered in figure 6. The basic problem is to account for the shading of one leg by the other. The radiation between cylinder X (fig. 6) and quadrants 1 and 2 of the lunar plain should be exactly one-half that received between a vertical cylinder and the entire plain. The discussion here is, again, limited to the case in which the lunar plain is taken as infinite. Since the head was exposed to radiation from the full plain, for the leg and the half-plain

$$F_{1,2} = 0.25 \tag{15}$$

The radiation between quadrants 3 and 4 and cylinder X is partially blocked by cylinder Y. The projected length of the circumference of cylinder X viewed from quadrants 3 and 4 is D cos θ (appendix A). Thus, $A_p = DH \sin\phi \cos\theta$, and

$$F_{3,4} = \frac{2DH}{\pi DH} \int_{\theta=0}^{\pi/2} \int_{r=0}^{\infty} \frac{\cos\phi \sin\phi \cos\theta\, r\, dr\, d\theta}{\pi\rho^2} = 0.5\pi = 0.159 \tag{16}$$

The total for one leg is then

$$F_{leg} = (0.25 + 0.5\pi) = 0.409 \tag{17}$$

Total body. - To determine the heat exchange for the entire multicylinder body, the values of $\overline{F}$ obtained for the parts of the body are multiplied by the percentage of the total surface area contributed by each member, and the results are summed. For the proportions shown in figure 2, the result is, for the infinite lunar plain

$$F = 0.463 \tag{18}$$

Effects on the Hemisphere-Cylinder Man

The serious disadvantage in using the multicylinder man for heat evaluations is the difficulty in determining the projected areas of its various members. A simple geometric configuration having a shape factor F closely approximating that of the multicylinder man is a right circular cylinder body capped with a hemisphere head (fig. 7).

For the head (fig. 8), the projected area A_p to be used with the parallel-ray shape factor analysis, as shown in appendix B, is

$$A_p = \frac{\pi a^2}{2}(1 - \cos \phi) \tag{19}$$

so that, for the infinite plain

$$F_{head} = \frac{4}{2\pi a^2} \int_{\theta=0}^{\pi/2} \int_{r=0}^{\infty} \frac{\cos \phi}{\pi \rho^2} \frac{\pi a^2}{2} (1 - \cos \phi) r \, dr \, d\theta = 0.25 \tag{20}$$

The result determined for the head of the multicylinder man may be used for the body of the hemisphere-cylinder man

$$F_{body} = 0.5 \tag{21}$$

Taking the height of the cylinder to be 5 feet and the diameter to be 1.52 feet, the cylinder is 86.5 percent and the hemisphere 13.5 percent of the total surface area. Multiplying these percentages by the respective values of F and combining the results yields a total value for the entire hemisphere-cylinder man

$$F = 0.865 \times 0.5 + 0.135 \times 0.25 = 0.466 \tag{22}$$

This value is seen to be quite close to that obtained for the more complex multicylinder man (eq. (17)). Therefore, the simpler hemisphere-cylinder man is used in subsequent analyses.

SOLAR RADIATION EFFECTS

In the foregoing analysis, the effects of solar radiation upon the multicylinder man and upon the lunar surface have not been considered. The moon is a planetoid, and its only significant source of heat is the sun. Therefore, the lunar temperature at any point is a function of the incident solar radiation. Because of the relatively slow moon rotational speed, the temperature attained at any point on the surface is approximately the equilibrium temperature. To determine a temperature profile for the lunar equator, the solar flux distribution must be obtained. (The lunar equator will be considered the locus of subsolar points. The equator is actually 1°32' from the ecliptic.)

An energy balance between the absorbed and the emitted energy on the moon surface gives $e = G_n(1 - a)$, in which G_n is the solar flux normal to the surface, e is the lunar emissive power, and a represents the moon's albedo or the proportion of sunlight which is reflected. If G_s represents the solar constant (the normal flux at the subsolar point), then a factor F_s may be defined

$$F_s = \frac{G_n}{G_s} \tag{23}$$

If θ represents the longitude measured from the dawn point, F_s should be $\sin\theta$. However, in such an instance at $\theta = 0°$, $F_s = G_n = e = 0$. This does not agree with lunar observations. Lunar temperature curves (ref. 4) yield $e_0 = 16$ Btu/hr-ft^2 and $e_{90} = 410$ Btu/hr-ft^2. Thus, in this work $F_s = \sin\theta$ is presumed to hold near the subsolar point, and this variation is allowed to blend into a tangent straight line such that, at $\theta = 0°$

$$F_s = \frac{e_0}{e_{90}} = \frac{16}{410} = 0.039 \tag{24}$$

This representation is not unlike that used in reference 5.

The requirement that $e_{90} = 410$ Btu/hr-ft^2 is satisfied by taking the albedo, $a = 0.07$. These facts are illustrated in figure 9 and result in

$$e = G_s F_s (1 - a) \tag{25}$$

$$G_s = 440 \text{ Btu/hr-ft}^2 \tag{26}$$

$$a = 0.07 \tag{27}$$

$$F_s = \sin \theta \tag{28}$$

where $28.26° \leq \theta \leq 90°$, and

$$F_s = 0.039 + 0.880\theta \tag{29}$$

where $0° \leq \theta \leq 28.26°$.

The constants in equations (25) to (29) were obtained by matching, analytically, the slopes of the sine curve and the straight line. The temperature profile, as a function of position along the equator, may be obtained from $e = \epsilon_m \sigma T^4$, where ϵ_m is the lunar surface emissivity. The temperature profile which results when $\epsilon_m = 1.0$ is plotted in figure 10.

The lunar-flux profile determined in figure 9 makes possible the calculation of the total heat absorbed by a hemisphere-cylinder man as his position on the lunar plain varies from the subsolar point to the dawn point. The total radiant heat per unit of surface area at various positions between these two points is plotted in figure 11. The infrared total hemispheric emissivity ϵ and the solar absorptivity α_s of the surface of the man were assigned values of 0.05, 0.15, 0.13, 0.5, 0.7, 0.85, and 0.95; and 0.1, 0.15, 0.2, and 0.3, respectively. A figure was drawn for each absorptivity, and ϵ as the parameter was allowed to vary over the range of 0.05 to 0.95 (fig. 11).

These curves were calculated from the following relationship, which is derived in appendix C.

$$\frac{q_{abs}}{A_t} = G_s \left\{ \alpha_s F_m + \left[\epsilon(1 - a) + \alpha_s a \right] FF_s \right\} \tag{30}$$

Definitions have been given for G_s, α_s, ϵ, a, F, and F_s. The total radiant heat absorbed by the man is q_{abs}, and A_t is the total surface area. The factor F_m represents the ratio between the projected surface area of the man, normal to the sun's rays, and the total surface area A_t. For the hemisphere-cylinder man

$$F_m = \frac{\frac{1}{\pi}\cos\theta + 0.125\frac{D}{H}(1 + \sin\theta)}{1 + 0.5\frac{D}{H}} \tag{31}$$

The preceding analysis, which showed that the value of F (between the lunar surface and the man) obtained for either a multicylinder man or a hemisphere-cylinder man were essentially the same, was based on the parallel-ray approximation developed in the section entitled "Thermal Radiation Concepts." Since the solar irradiation is of a parallel-ray nature, it is expected that the value of F_m given in equation (31) for the hemisphere-cylinder man would not differ from that which would be obtained for the multicylinder man if shadowing effects are ignored.

In calculating the results shown in figure 11, the data given in equations (22), (25) to (29), and (31) were used in equation (30). The dimensions used for H and D were 5.0 feet and 1.52 feet, respectively. Equation (30) may be used for other assumed configurations of the man, but appropriate relations for F and F_m must be found.

The curves in figure 11 illustrate that for $\epsilon = 0.05$, the man receives more heat at the dawn point $\theta = 0°$ than at the subsolar point $\theta = 90°$. This is caused by the relatively small emphasis placed on lunar heat by the ϵ value of 0.05. For other ϵ values considered, however, more heat is received at the subsolar point than at the dawn point.

All curves indicate a value of θ for which the heat absorbed by the man is greatest. This angle of maximum heat absorption may be determined analytically from equation (30) when the appropriate relations for F, F_m, and F_s are used. These relations are derived in appendix C and applied to the hemisphere-cylinder man. The results show that the angle of maximum absorption $\theta_{q_{max}}$ is dependent, for a given geometry, only on the ratio α_s/ϵ. This relation is plotted in figure 12 and, in a more directly usable form, in figure 13. As α_s/ϵ decreases, the point of maximum heat absorption moves from near subsolar points toward the dawn point.

HEAT CONDUCTED THROUGH SURFACE INSULATION

The quantity of heat absorbed by the outer skin and conducted through the insulation of the hemisphere-cylinder man is dependent upon the magnitude of absorbed

radiation, the emissivity ϵ of the outer skin, and the thermal conductivity k and thickness Δx of the insulating material. (See fig. 14.)

A heat balance for the insulating material on the man gives

$$\frac{q_{abs}}{A_t} = \frac{q_r}{A_t} + \frac{q_c}{A_t} \tag{32}$$

where q_r and q_c represent the heat radiated by the surface and the heat conducted into the interior, respectively. Thus

$$\frac{q_r}{A_t} = \epsilon\sigma T^4 \tag{33}$$

and

$$\frac{q_c}{A_t} = \frac{k}{\Delta x}\left(T - T_i\right) \tag{34}$$

where T_i is the inner skin temperature of the insulation. Then

$$\frac{q_{abs}}{A_t} = \epsilon\sigma T^4 + \frac{q_c}{A_t} \tag{35}$$

For a given inner skin temperature, equations (34) and (35) can be solved together to eliminate the surface temperature T and yield a relation between the absorbed heat, the conducted heat, the surface emissivity, and the suit properties. Figure 14 was constructed in this manner.

In figure 14, the inner skin temperature was taken as 75° F. The curves were plotted over a range of values, with $k/\Delta x = U$ varying from 0.001 to 6.0 Btu/hr-ft^2-°F and ϵ ranging from 0.05 to 0.95. The curves show that for most values of ϵ and U there are corresponding values of the absorbed heat from which there is a negative conducted heat (heat flow from the inner to the outer skin). In addition, for each ϵ there is a value of the absorbed heat for which no heat is conducted through the insulation, that is, $T = T_i$. This zero-heat-leak condition occurs when $q_{abs}/A_t = \epsilon\sigma T_i^4$. In figure 15, this condition is plotted for $T_i = 75°$ F.

An example will best show the utilization of figure 14 with figure 11. The heat conducted through the insulation of a pressure-suited man is sought. The man's suit properties are $\alpha_s = 0.3$, $\epsilon = 0.7$, and $U = 6$ Btu/hr-ft^2-°F, if the man is standing at a position 30° from the dawn point. The energy the man absorbs is 107 Btu/hr-ft^2 (fig. 11(d)), and the heat conducted through the suit is 7.5 Btu/hr-ft^2 (fig. 14(n)).

THERMAL RADIATION FROM THE DARK PORTION OF THE MOON

The quantity of heat absorbed by a man on the dark portion of the moon is almost totally independent of the man's position. This is a result of the rapidity at which the moon dissipates its surface heat after sunset and of the length of the lunar night (14 earth days). The emission rate is assumed to be constant and equal to 2.63 Btu/hr-ft^2 (ref. 4). Since the absorbed thermal energy will be independent of the solar absorptivity of the suit in this instance, the α_s has been eliminated as an investigative parameter.

The technique used for the lunar-night evaluation is identical to that developed for the illuminated portion of the moon. The heat absorbed by the hemisphere-cylinder man is plotted in figure 16 for the range of emissivities previously considered. Figures 17(a) to 17(p) are plots of the conducted heat as a function of the absorbed heat for a wide range of overall heat-transfer coefficients. The utility of these figures is realized through correlation with figure 16, as demonstrated by the following example.

The heat conducted through the insulation of a pressure-suited man is sought. The suit properties are $\epsilon = 0.15$ and $U = 0.05$ Btu/hr-ft^2-°F, and the man is standing at a position 290° from the dawn point. The heat the pressure-suited man absorbs (fig. 16) is 0.610 Btu/hr-ft^2. A conducted heat of -10 Btu/hr-ft^2 is plotted in figure 17(g).

CONCLUDING REMARKS

The value of this paper lies in its ability to provide a quantitative evaluation of the effect of the lunar thermal environment on a pressure-suited man. Since the results of the investigations are presented in parametric form, the solution of specific problems over a wide range of variables is easily effected.

Interpretations and extrapolations are possible without loss of confidence in the results, if the basic premises are used as restraints. The more important postulates are: geometric simplifications of the man and the lunar surface are used; radiation and reflection are diffuse; conducted heat between the man and the lunar surface at the point of contact is not considered; the radiant characteristics of the suit and the overall

heat-transfer coefficient are unchanging over the man-model surface; and the effects of directly transmitted radiation (such as through a visor) are not considered.

Manned Spacecraft Center
National Aeronautics and Space Administration
Houston, Texas, August 16, 1967
914-80-05-01-72

NASA -S-67-5222

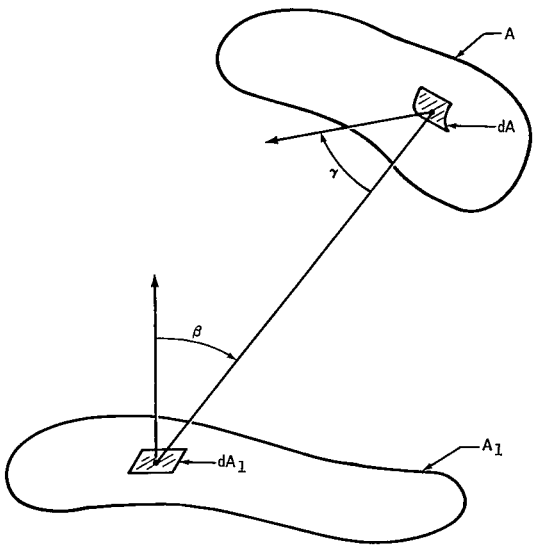

Figure 1. - Radiation exchange between finite areas.

NASA-S-67-5223

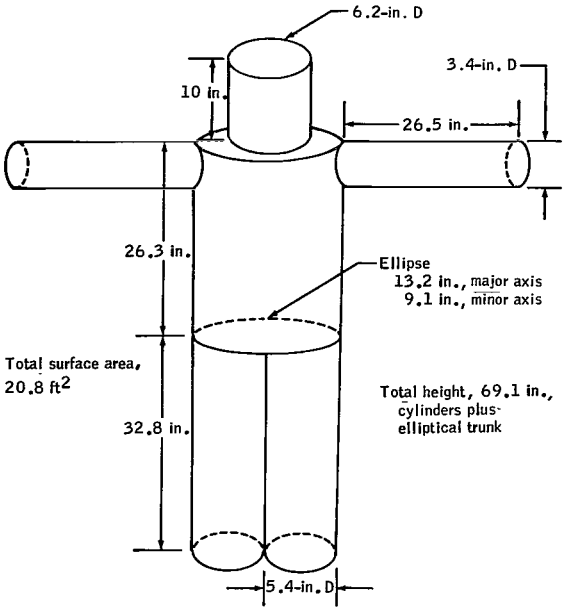

Figure 2. - Multicylinder man.

NASA-S-67-5224

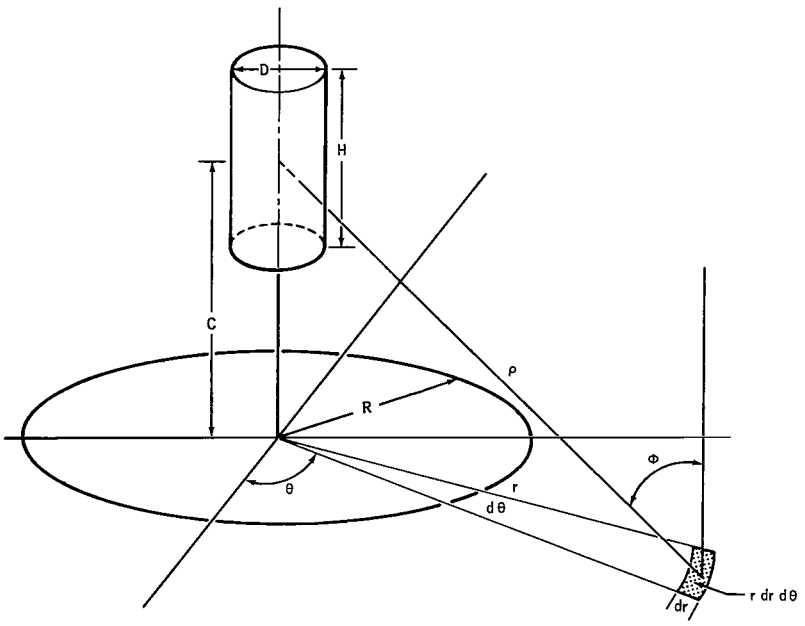

Figure 3. - Radiation from lunar plain to head.

NASA-S-67-5225

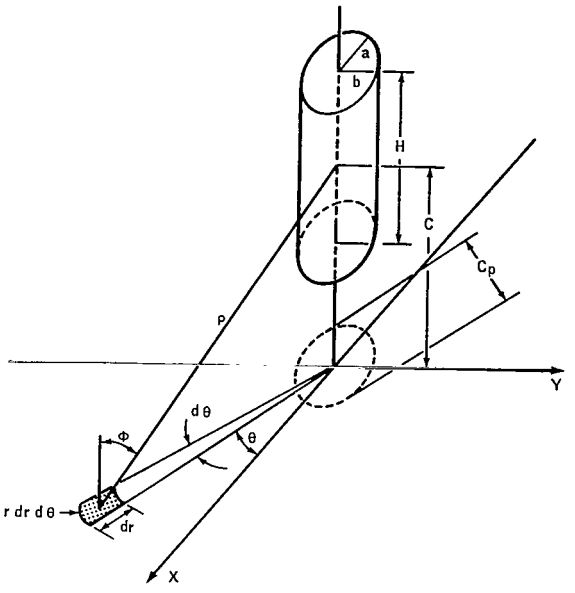

Figure 4. - Radiation from lunar plain to torso.

NASA-S-67-5226

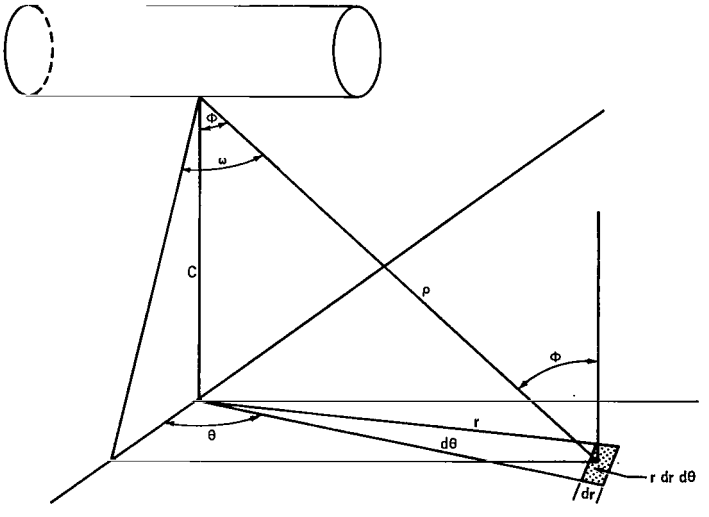

Figure 5. - Radiation from lunar plain to arm.

NASA-S-67-5227

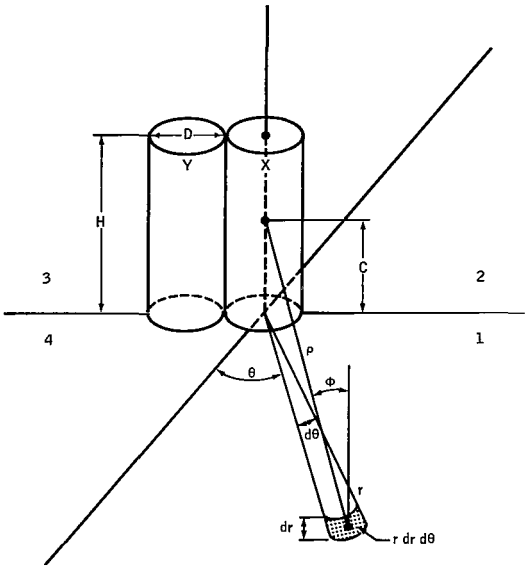

Figure 6. - Radiation from lunar plain to legs.

NASA-S-67-5228

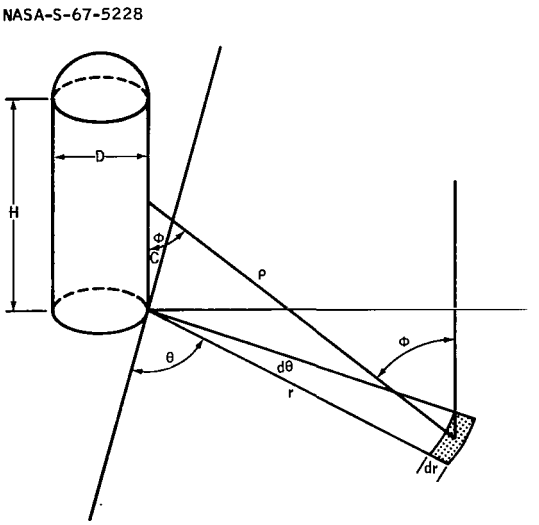

Figure 7. - Radiation from lunar plain to hemisphere-cylinder man.

NASA-S-67-5229

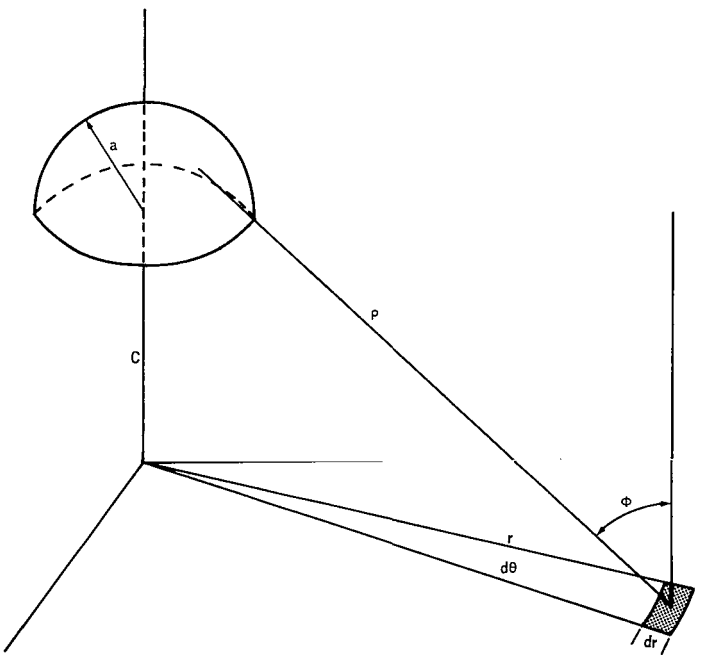

Figure 8. - Radiation from lunar plain to hemisphere.

NASA-S-67-5230

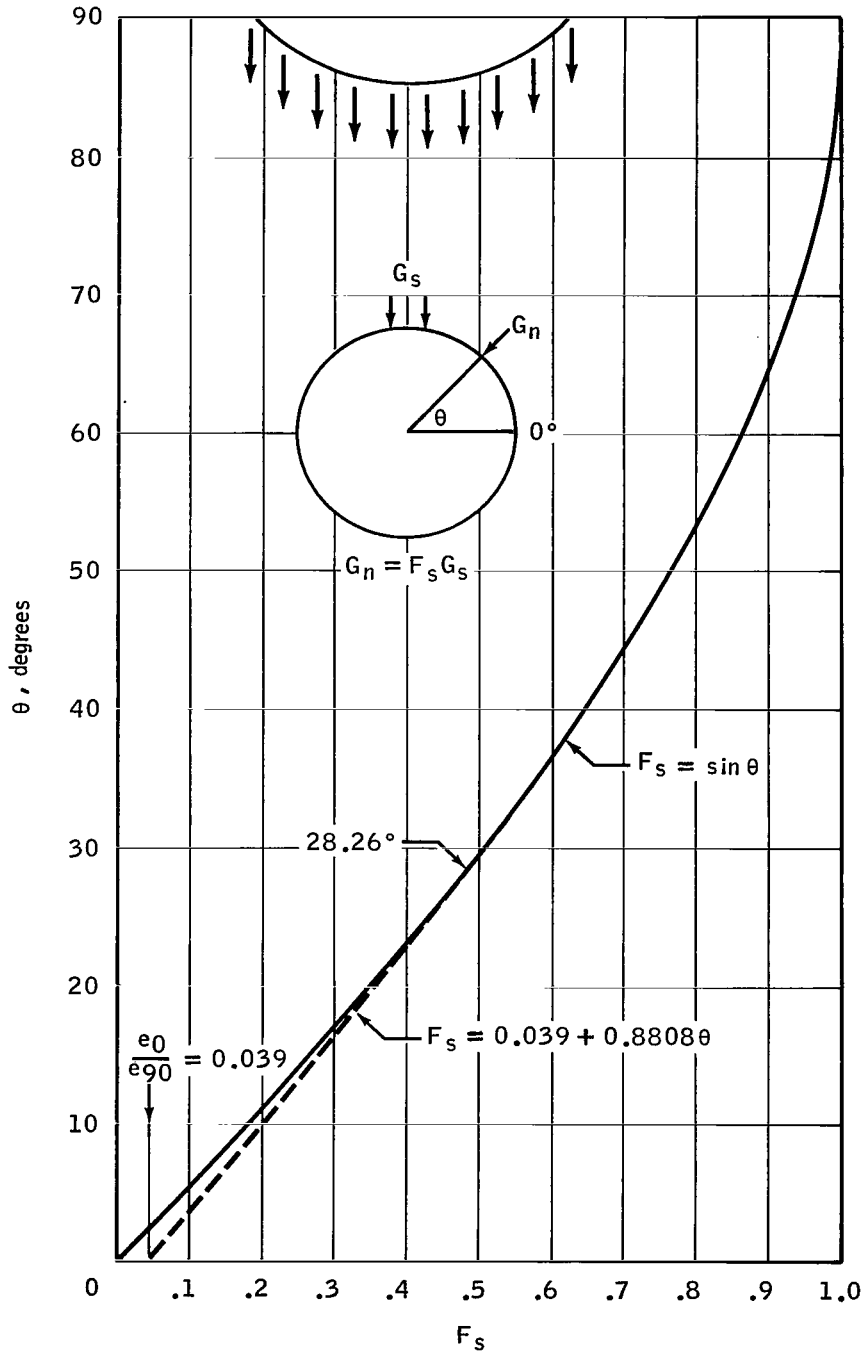

Figure 9. - Lunar surface solar view factor variance.

NASA-S-67-5231

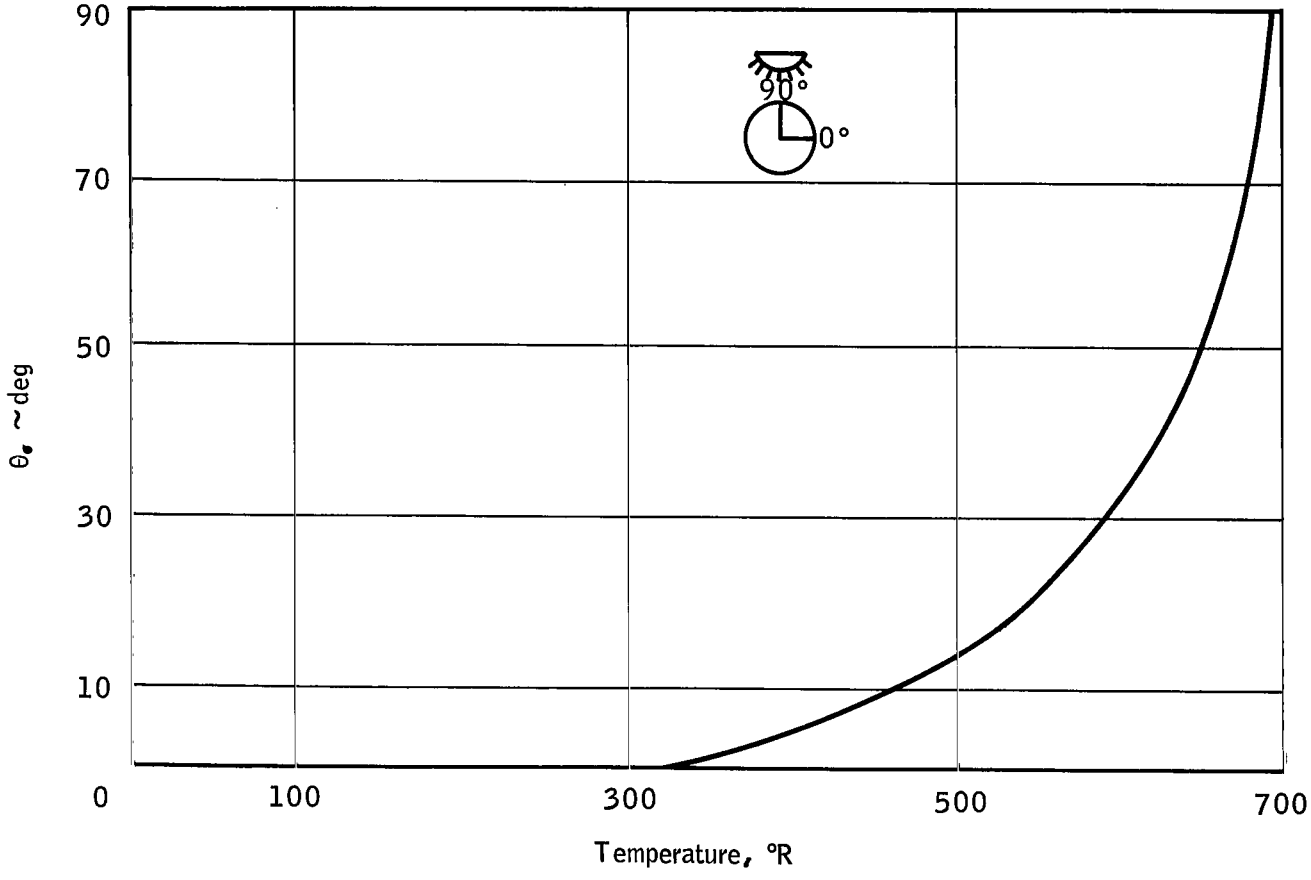

Figure 10. - Lunar temperature profile.

NASA-S-67-5232

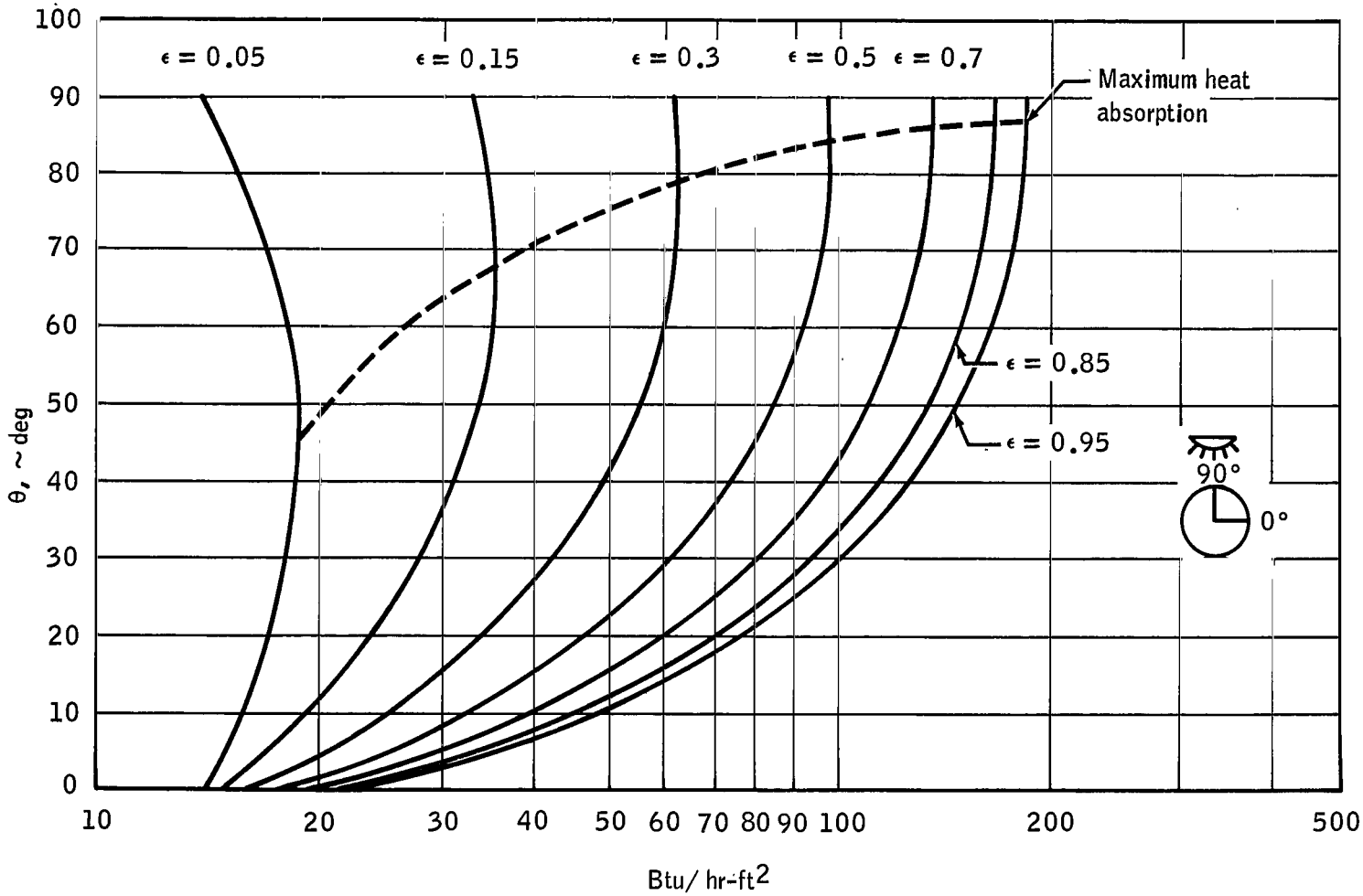

(a) $\alpha = 0.1$.

Figure 11. - Total heat absorption per unit of surface area.

NASA-S-67-5233

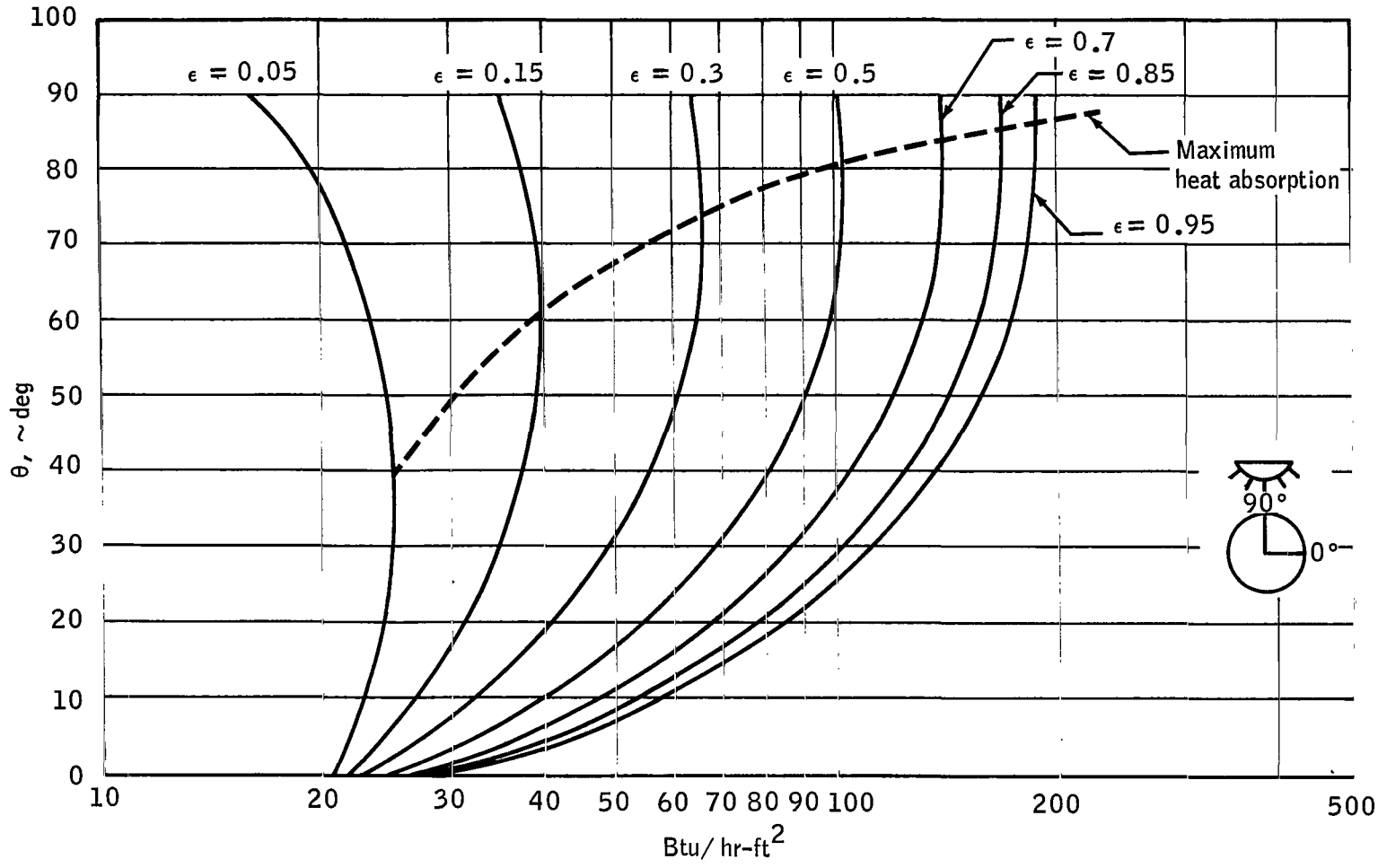

(b) $\alpha = 0.15$.

Figure 11. - Continued.

NASA-S-67-5234

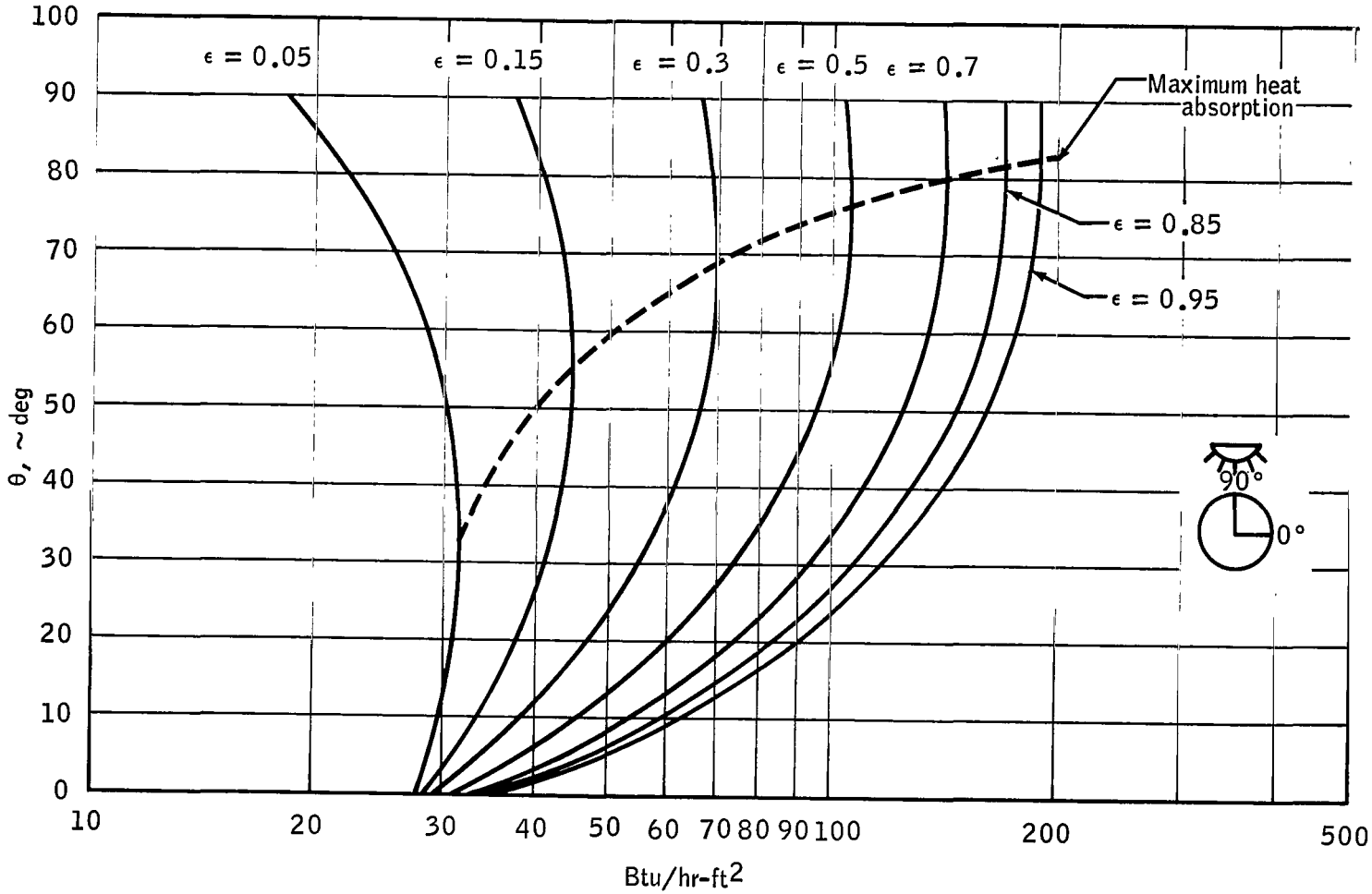

(c) $\alpha = 0.2$.

Figure 11. - Continued.

NASA-S-67-5235

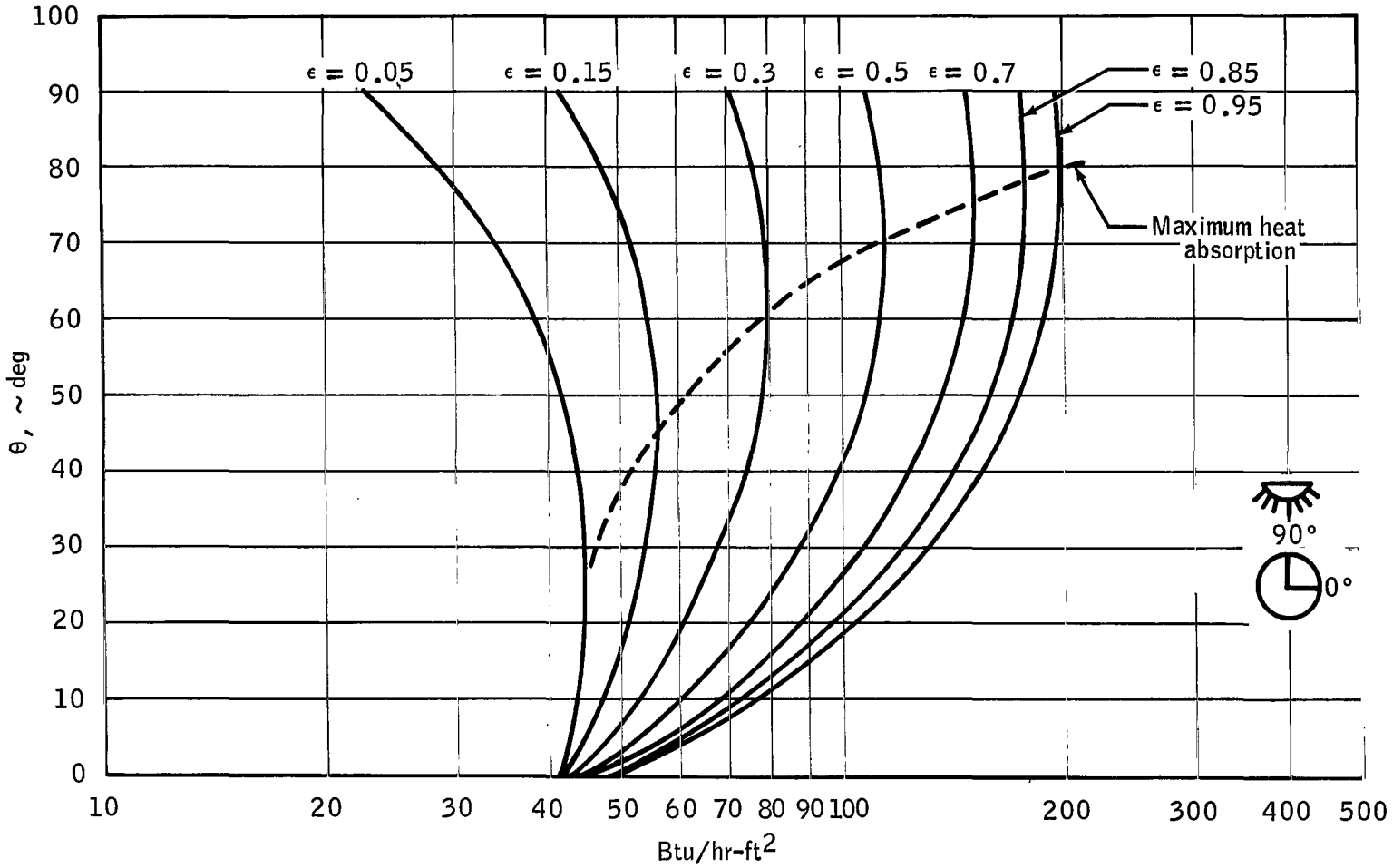

(d) $\alpha = 0.3$.

Figure 11. - Concluded.

NASA-S-67-5236

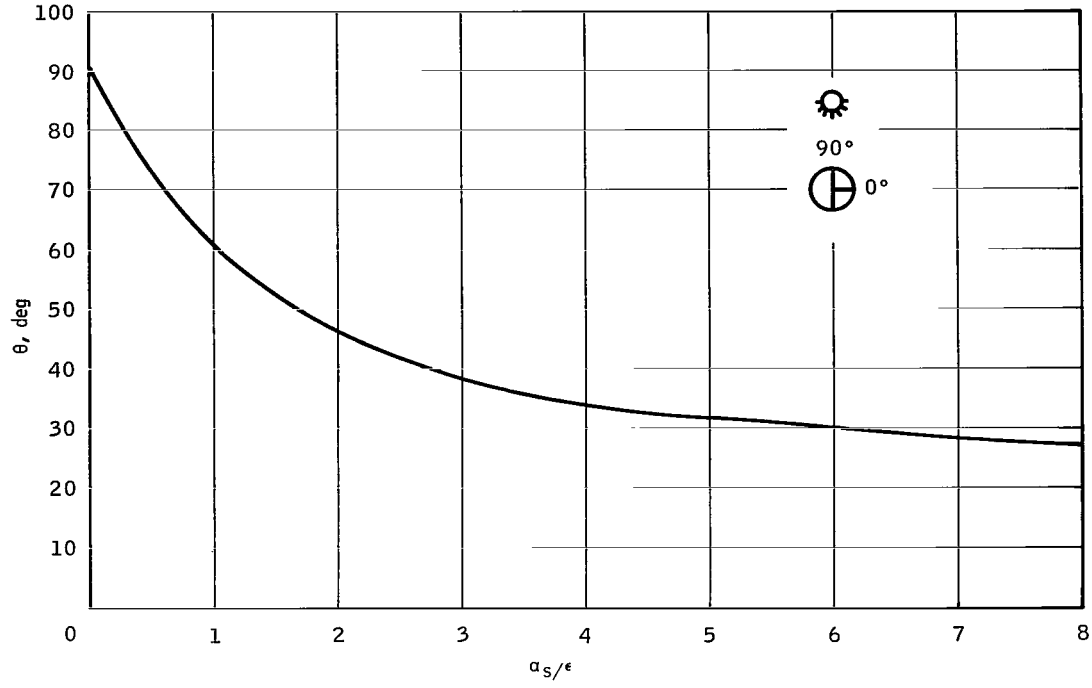

Figure 12. - Angle of maximum thermal load on the lunar surface.

NASA-S-67-5237

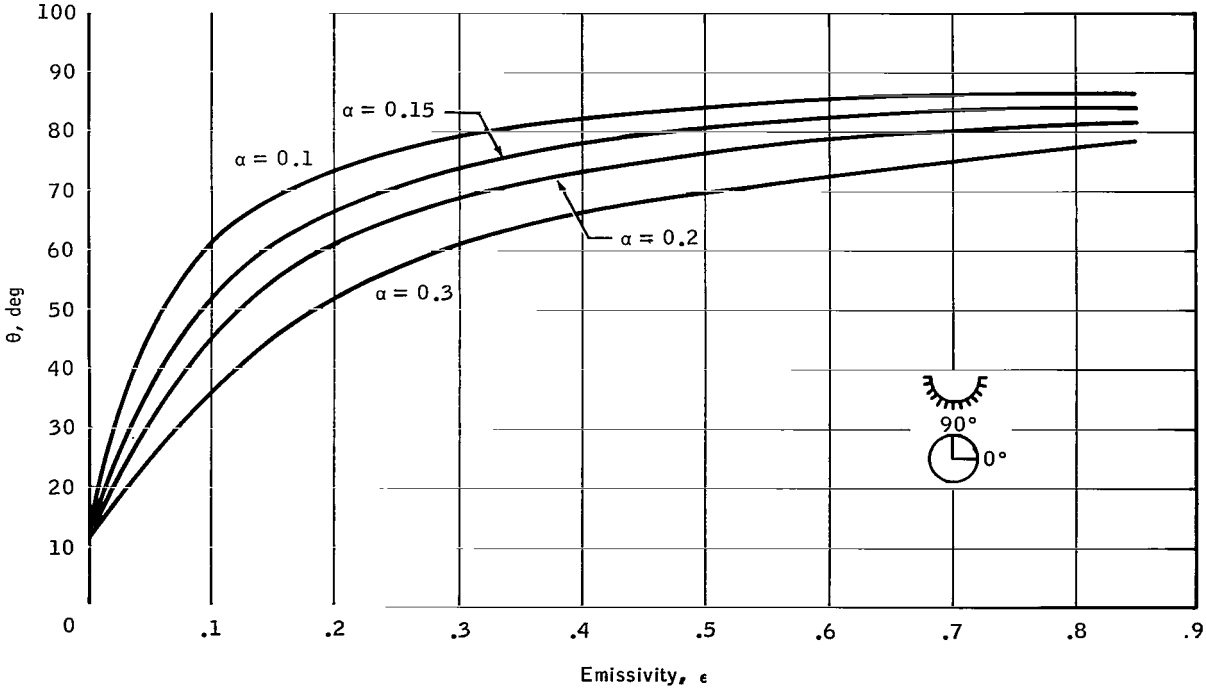

Figure 13. - Positions of maximum thermal load on the lunar surface.

NASA-S-67-5259

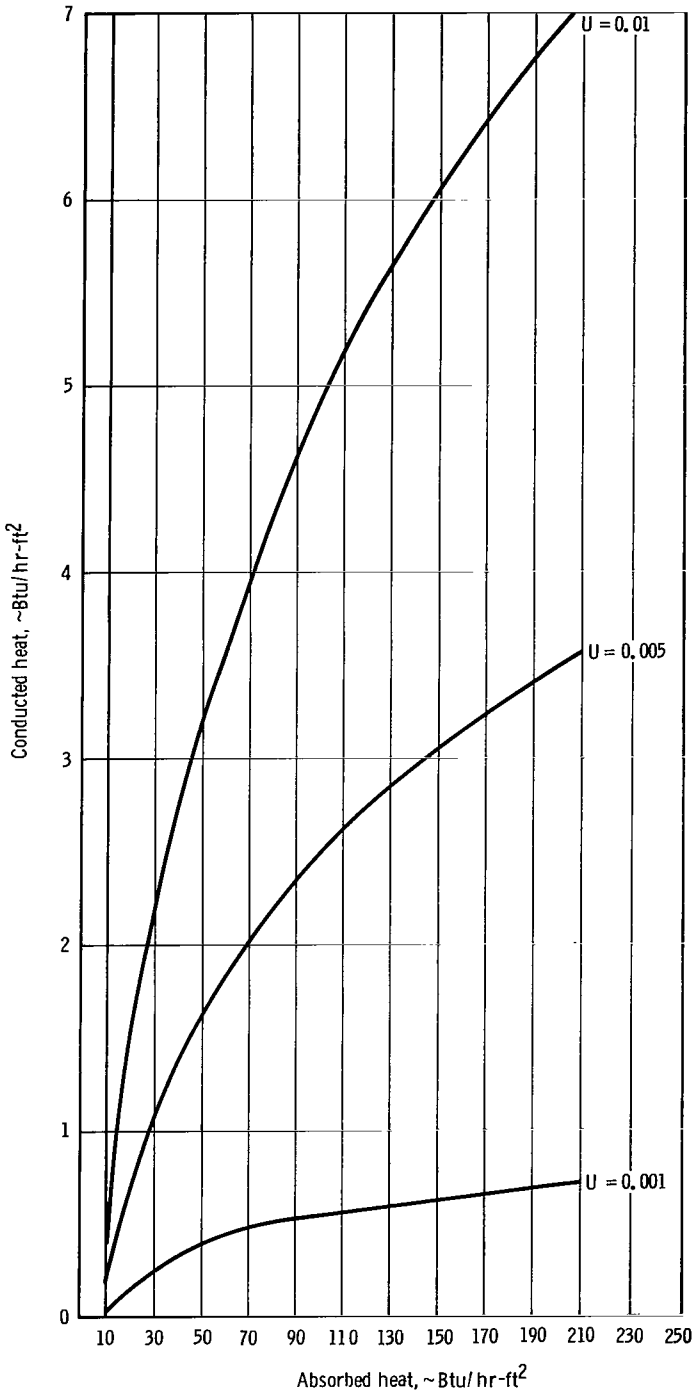

(a) U = 0.001 to 0.01, ϵ = 0.05.

Figure 14. - Plot of the relation between the absorbed heat, the conducted heat, the surface emissivity, and the suit properties.

NASA-S-67-5260

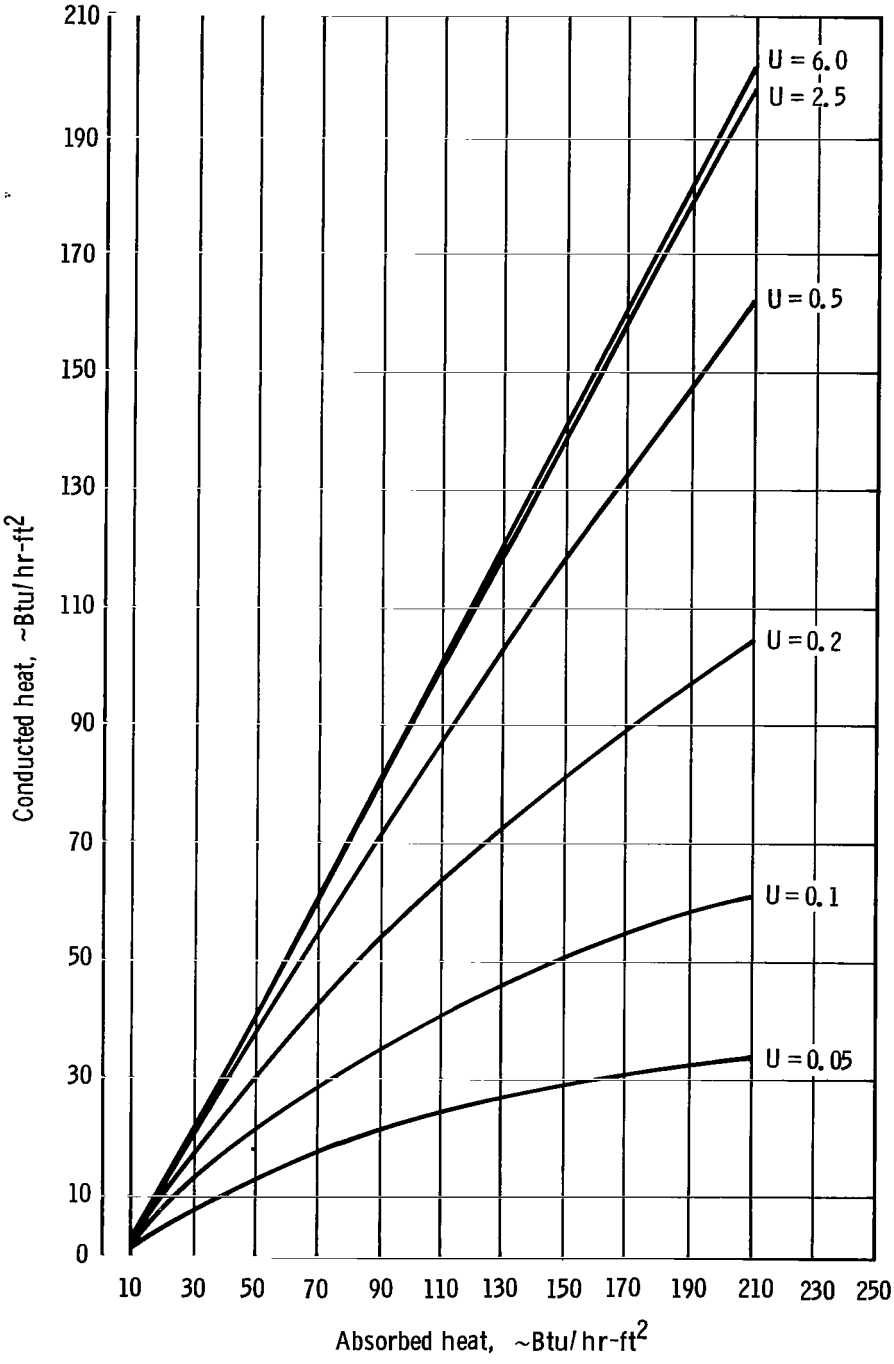

(b) U = 0.05 to 6.0, ϵ = 0.05.

Figure 14. - Continued.

NASA-S-67-5261

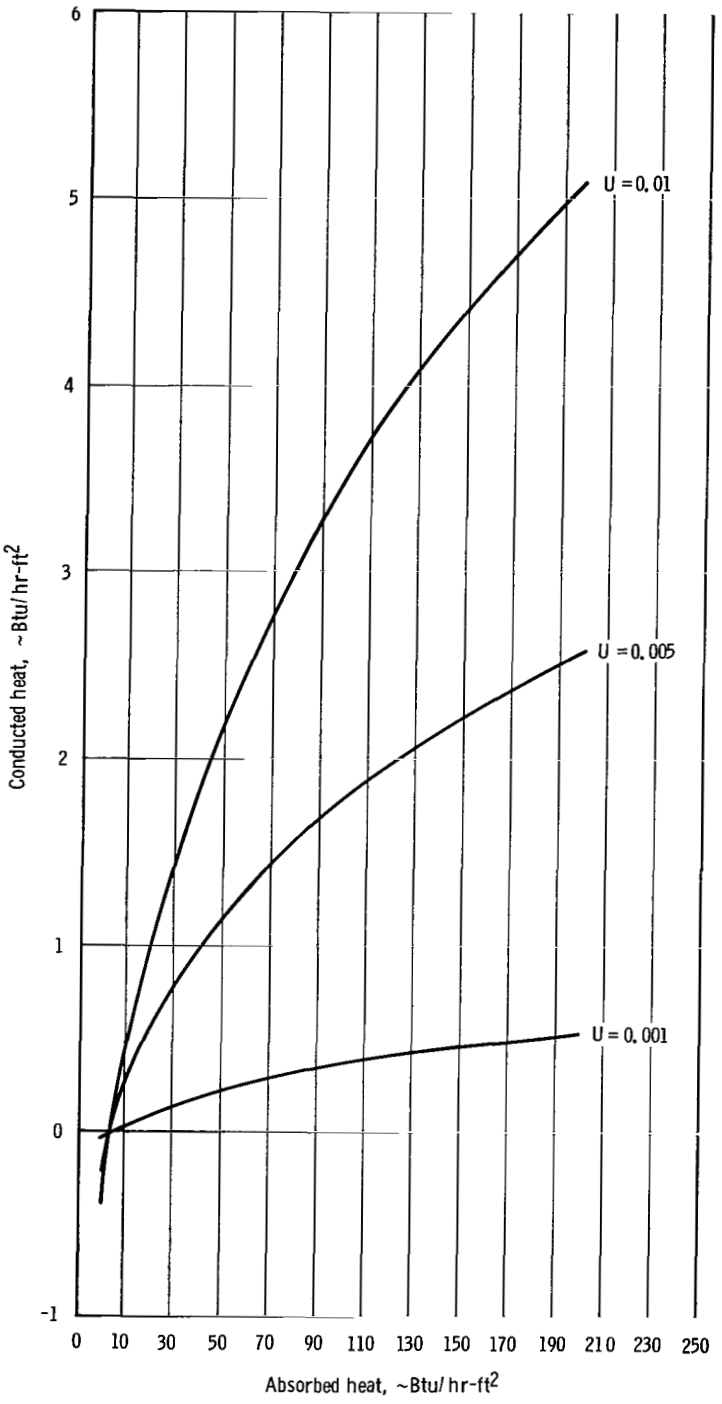

(c) U = 0.001 to 0.01, ϵ = 0.10.

Figure 14. - Continued.

NASA-S-67-5262

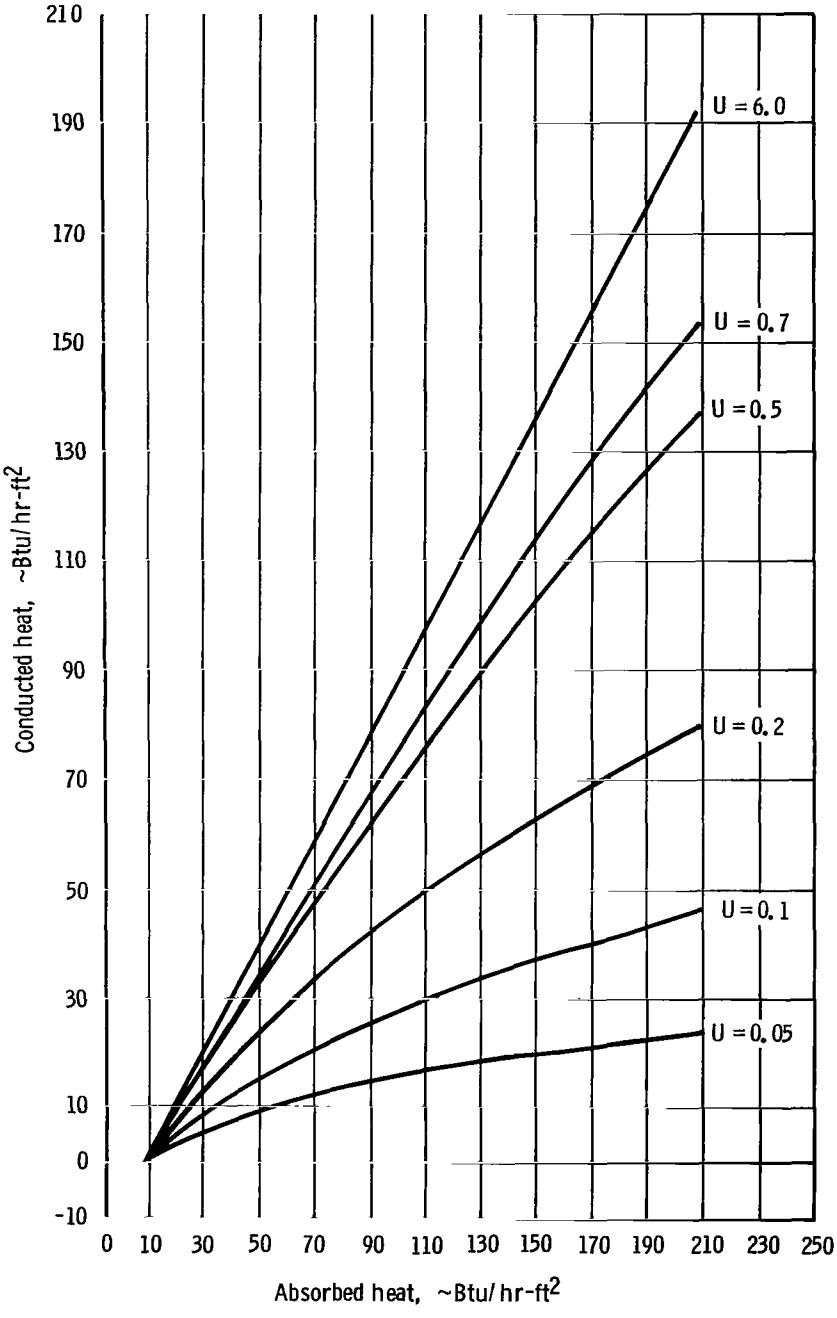

(d) U = 0.05 to 6.0, ϵ = 0.10.

Figure 14. - Continued.

NASA-S-67-5263

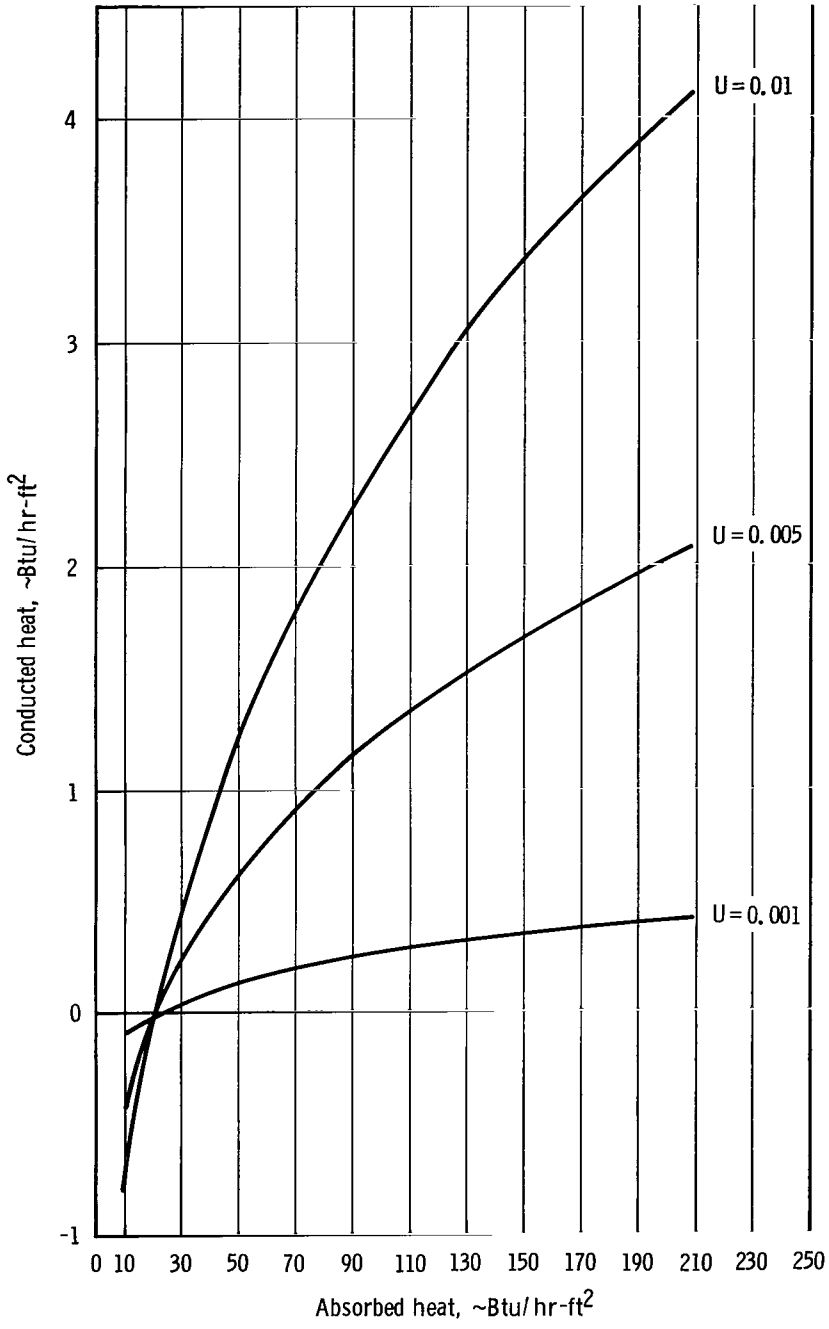

(e) U = 0.005 to 0.01, ϵ = 0.15.

Figure 14. - Continued.

NASA-S-67-5264

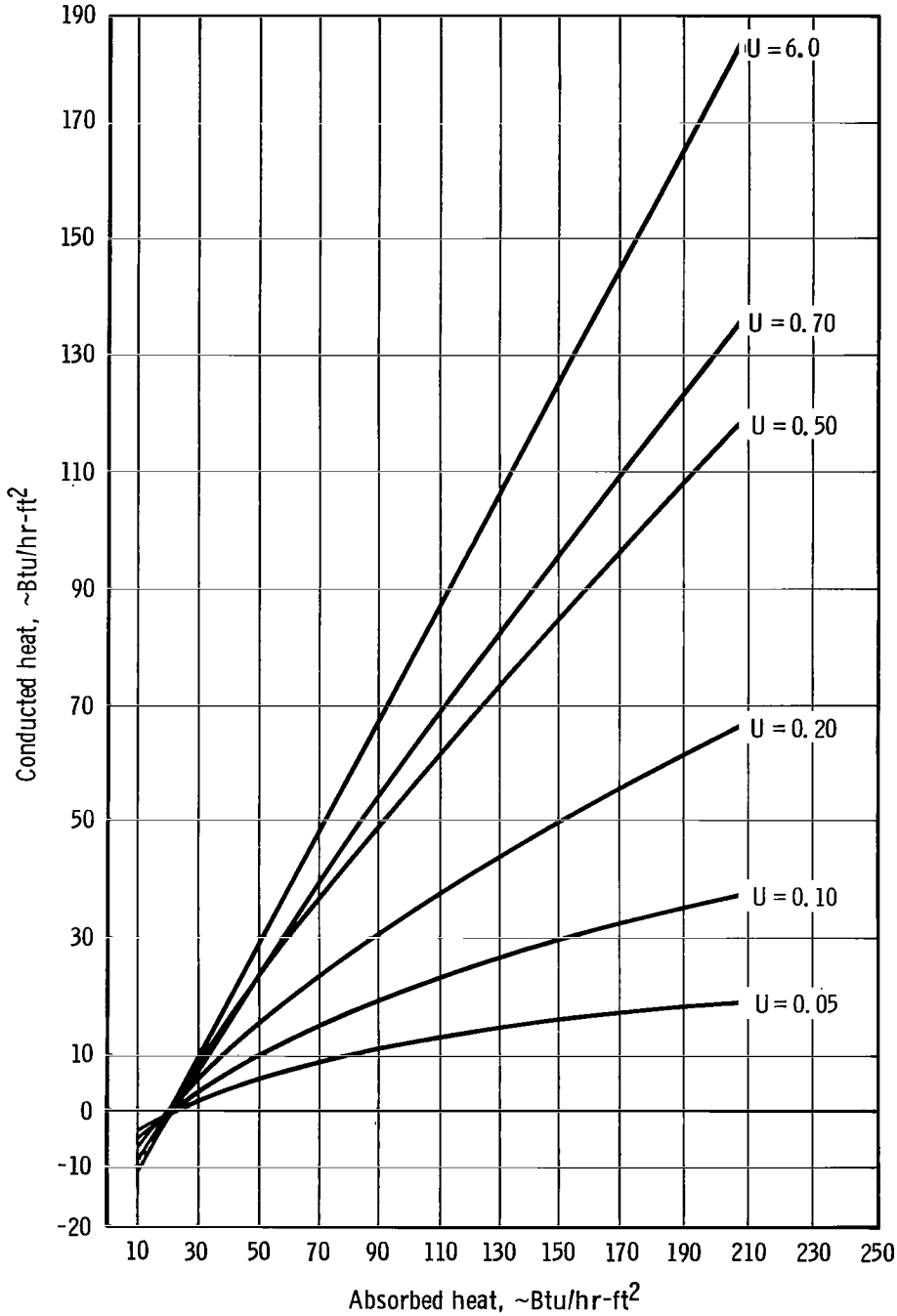

(f) U = 0.05 to 6.0, ϵ = 0.15.

Figure 14. - Continued.

NASA-S-67-5265

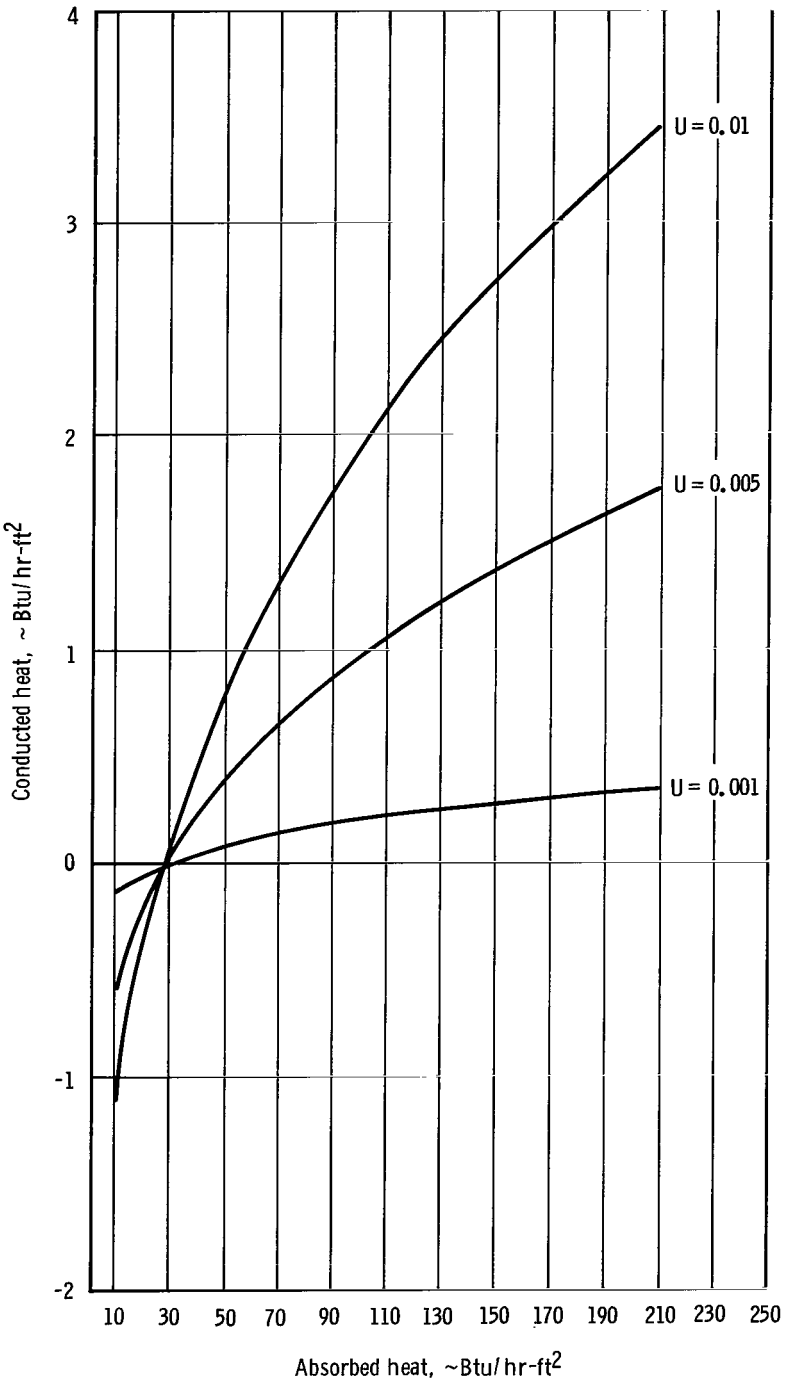

(g) U = 0.001 to 0.01, ϵ = 0.20.

Figure 14. - Continued.

NASA-S-67-5266

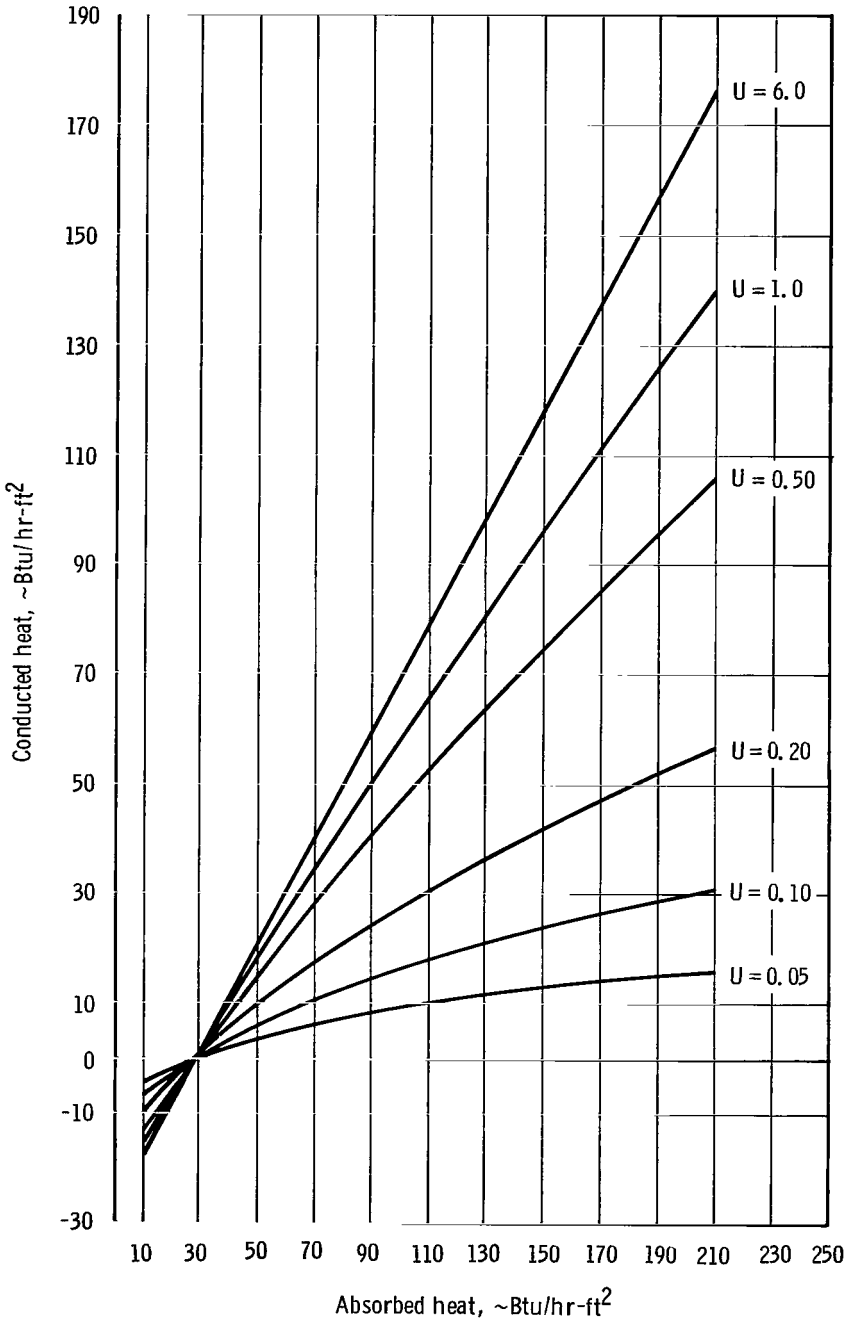

(h) U = 0.05 to 6.0, ϵ = 0.20.

Figure 14. - Continued.

NASA-S-67-5267

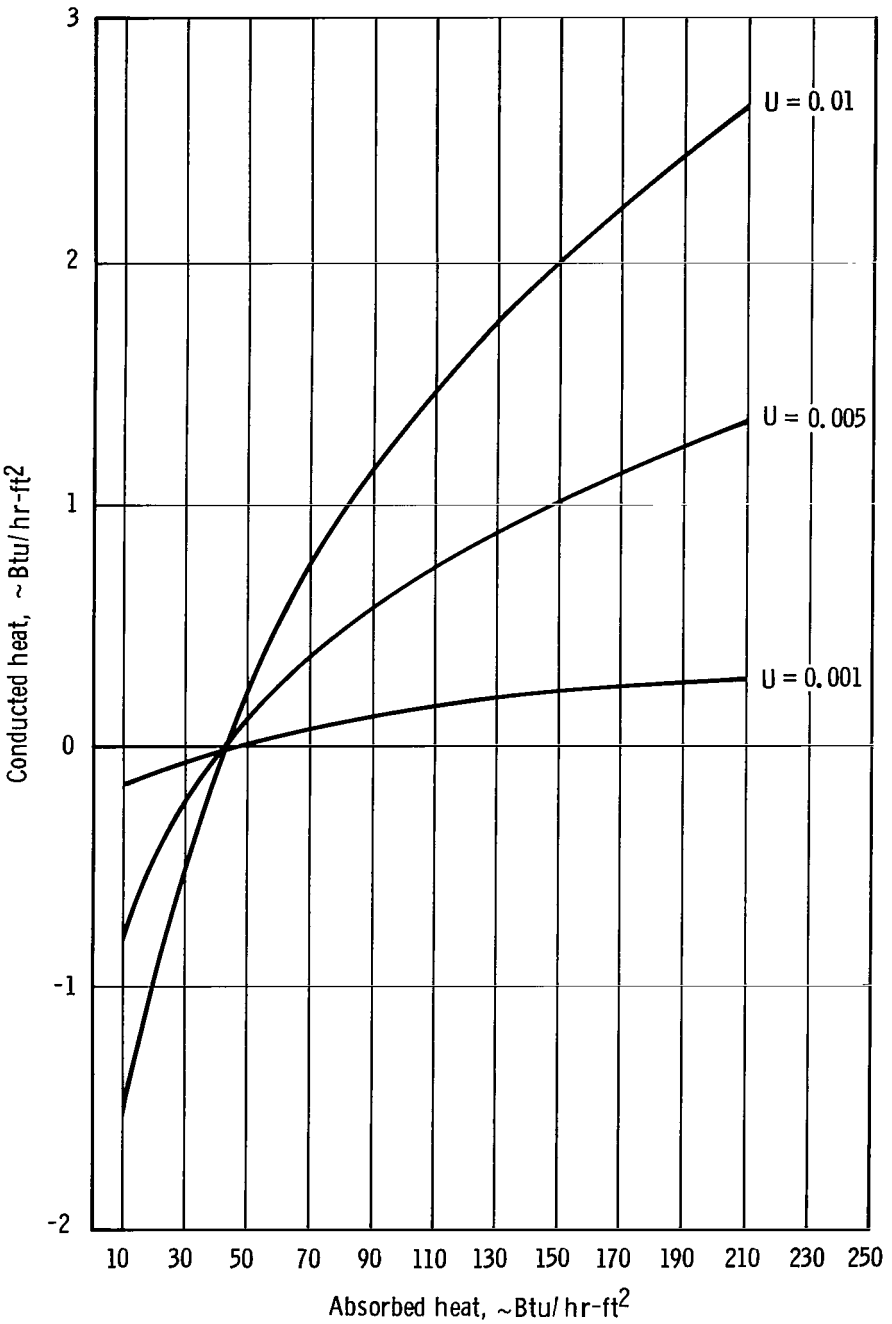

(i) U = 0.001 to 0.01, ϵ = 0.30.

Figure 14. - Continued.

NASA-S-67-5268

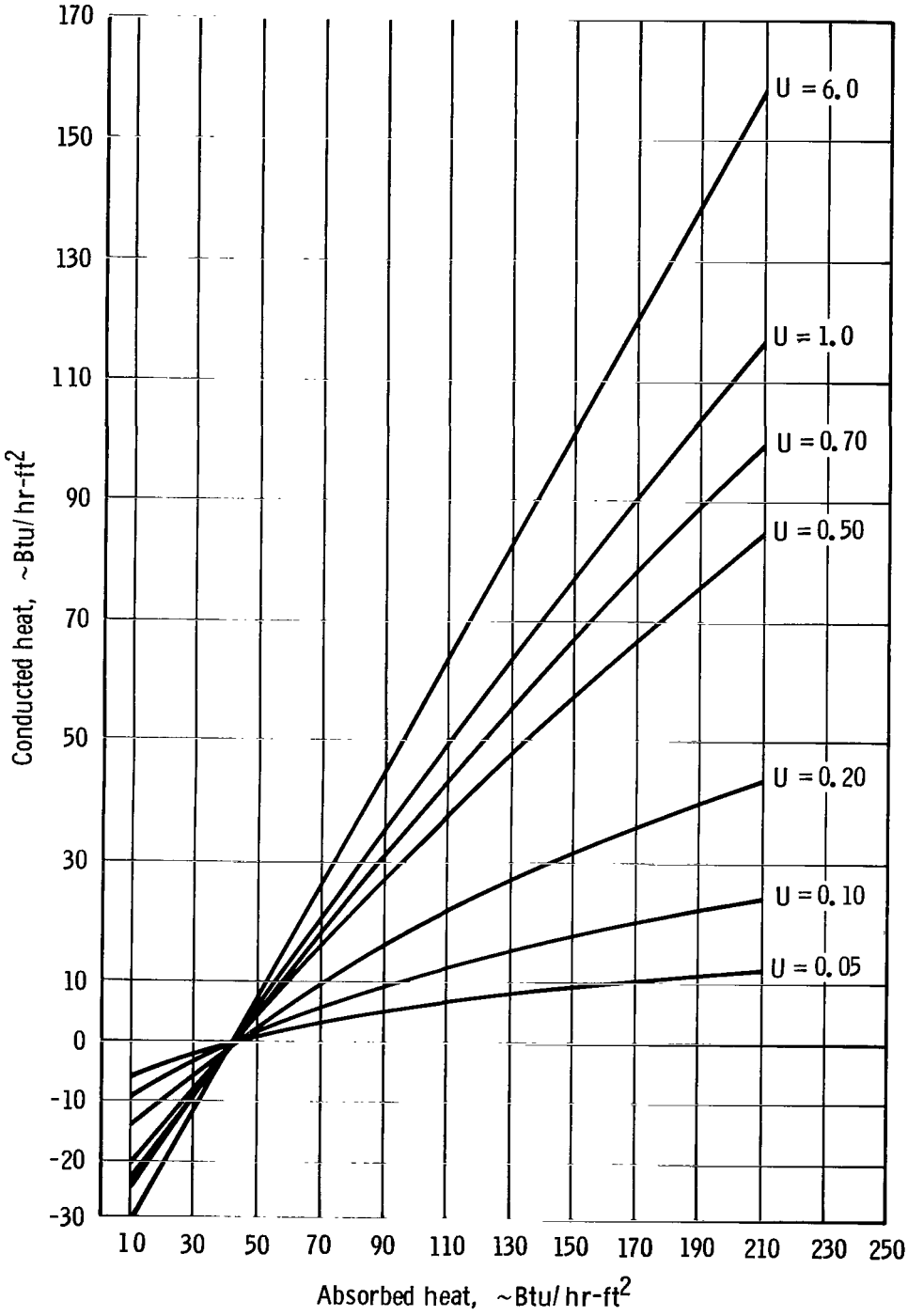

(j) U = 0.05 to 6.0, ϵ = 0.30.

Figure 14. - Continued.

NASA-S-67-5269

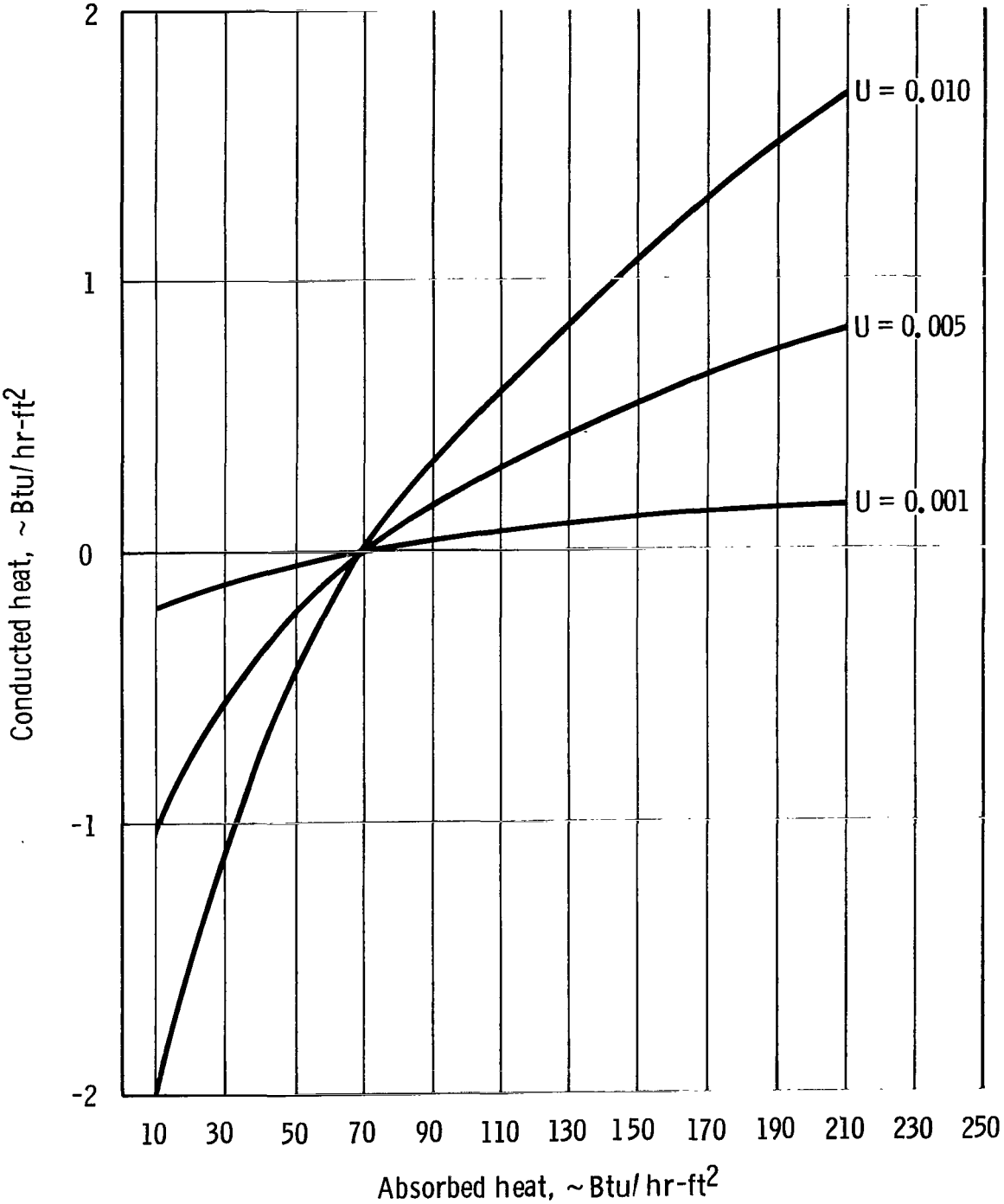

(k) U = 0.001 to 0.010, ϵ = 0.50.

Figure 14. - Continued.

NASA-S-67-5270

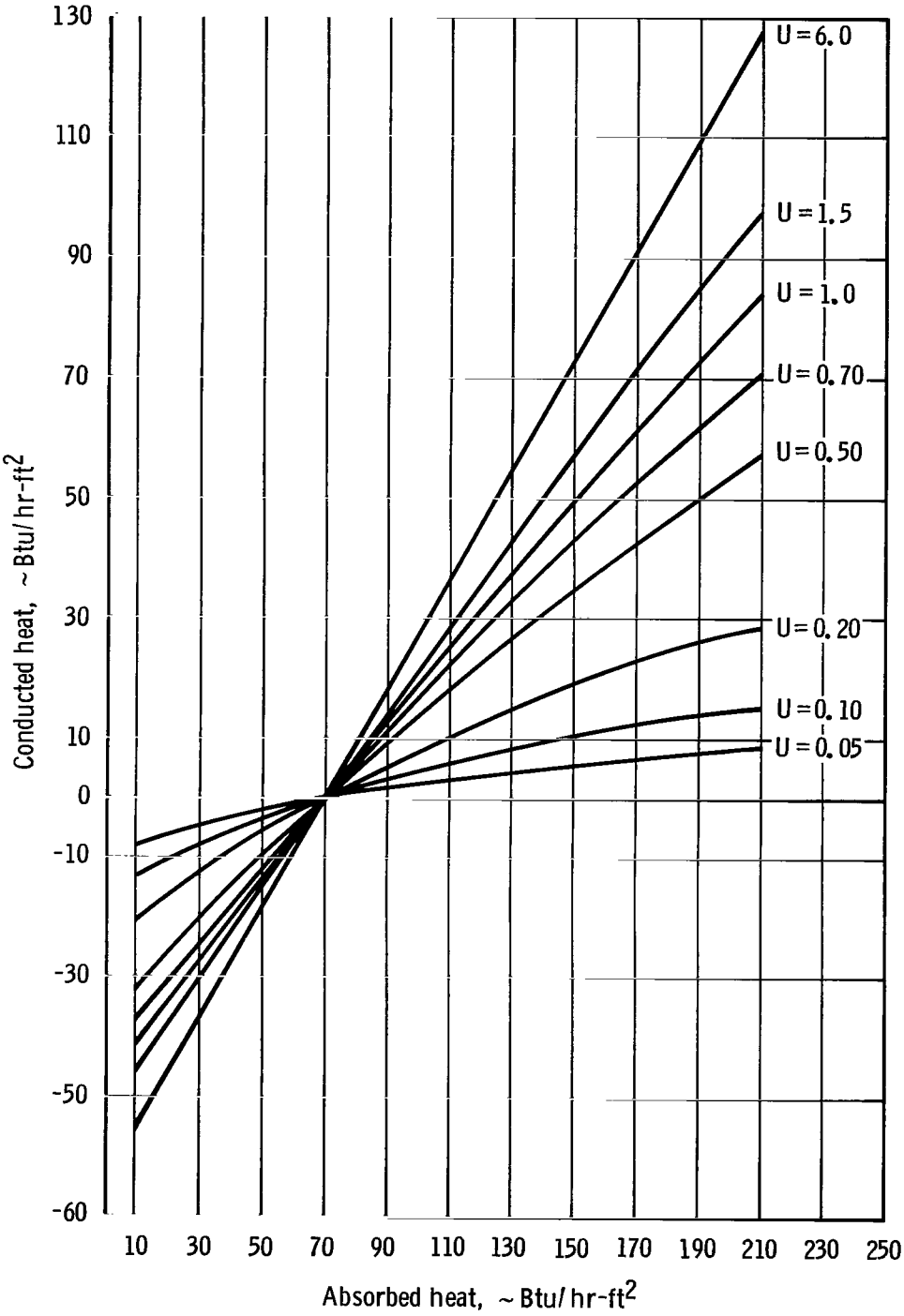

(1) U = 0.05 to 6.0, ϵ = 0.50.

Figure 14. - Continued.

NASA-S-67-5271

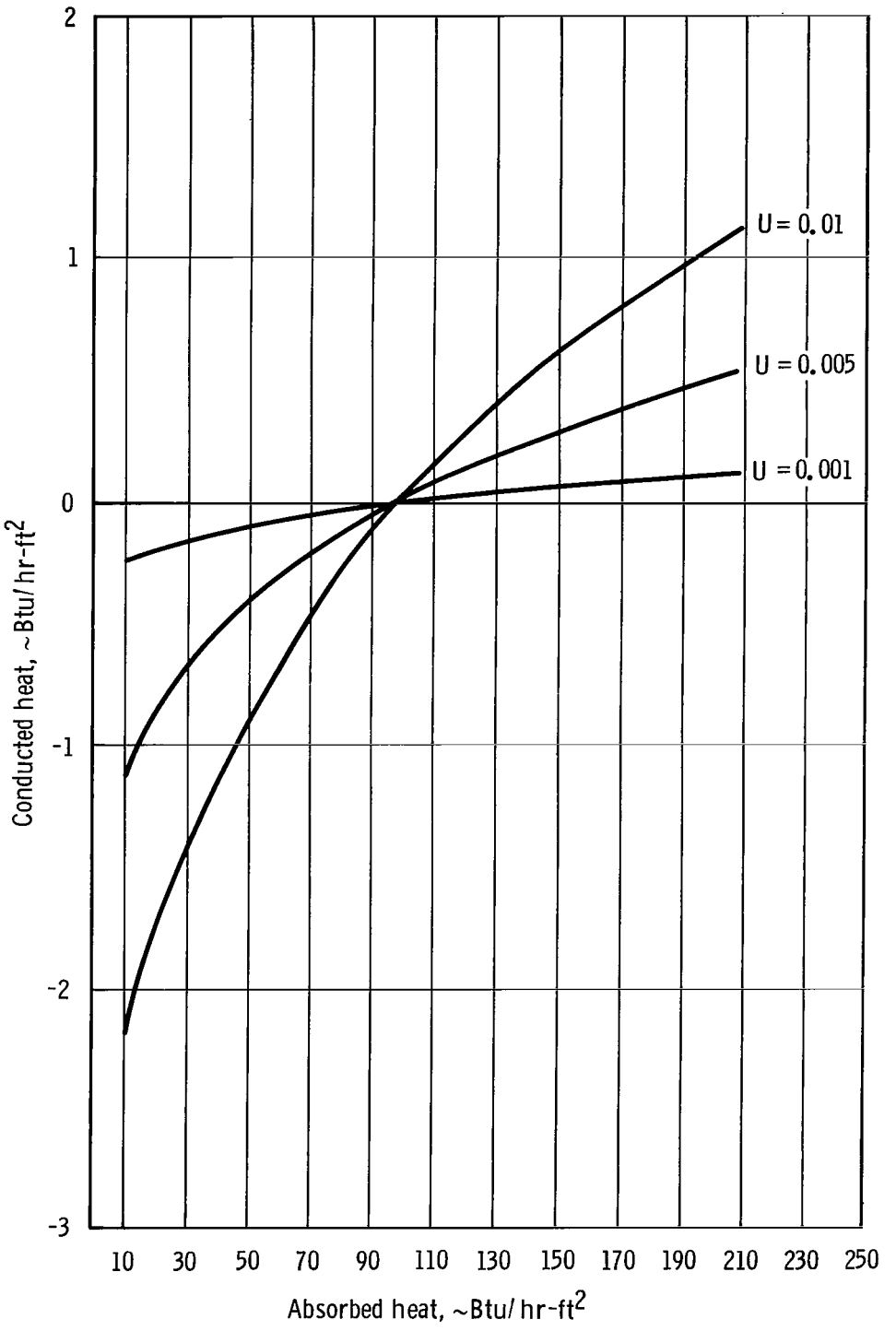

(m) U = 0.001 to 0.01, ϵ = 0.70.

Figure 14. - Continued.

NASA-S-67-5272

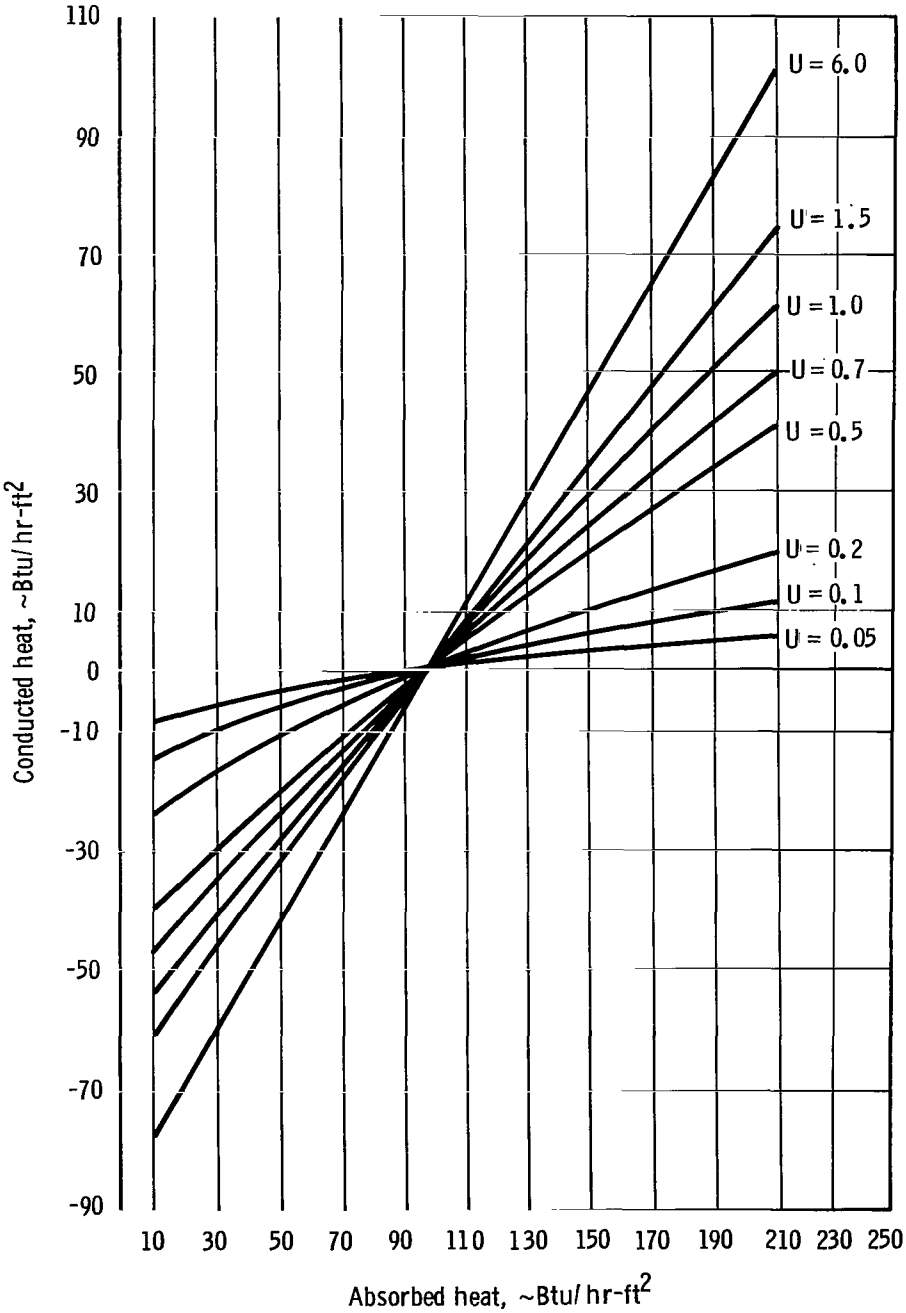

(n) U = 0.05 to 6.0, ϵ = 0.70.

Figure 14. - Continued.

NASA-S-67-5273

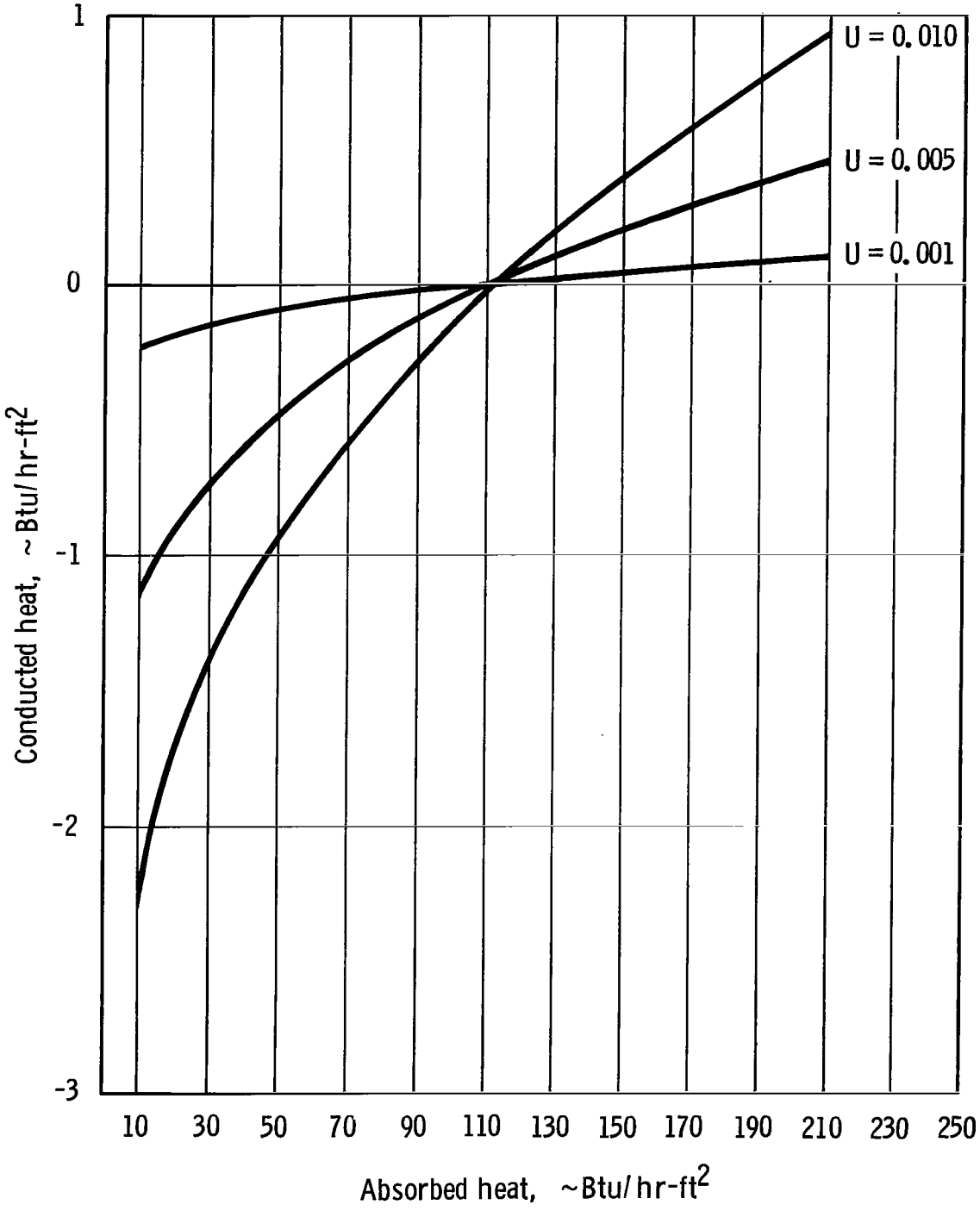

(o) U = 0.001 to 0.010, ϵ = 0.80.

Figure 14. - Continued.

NASA-S-67-5274

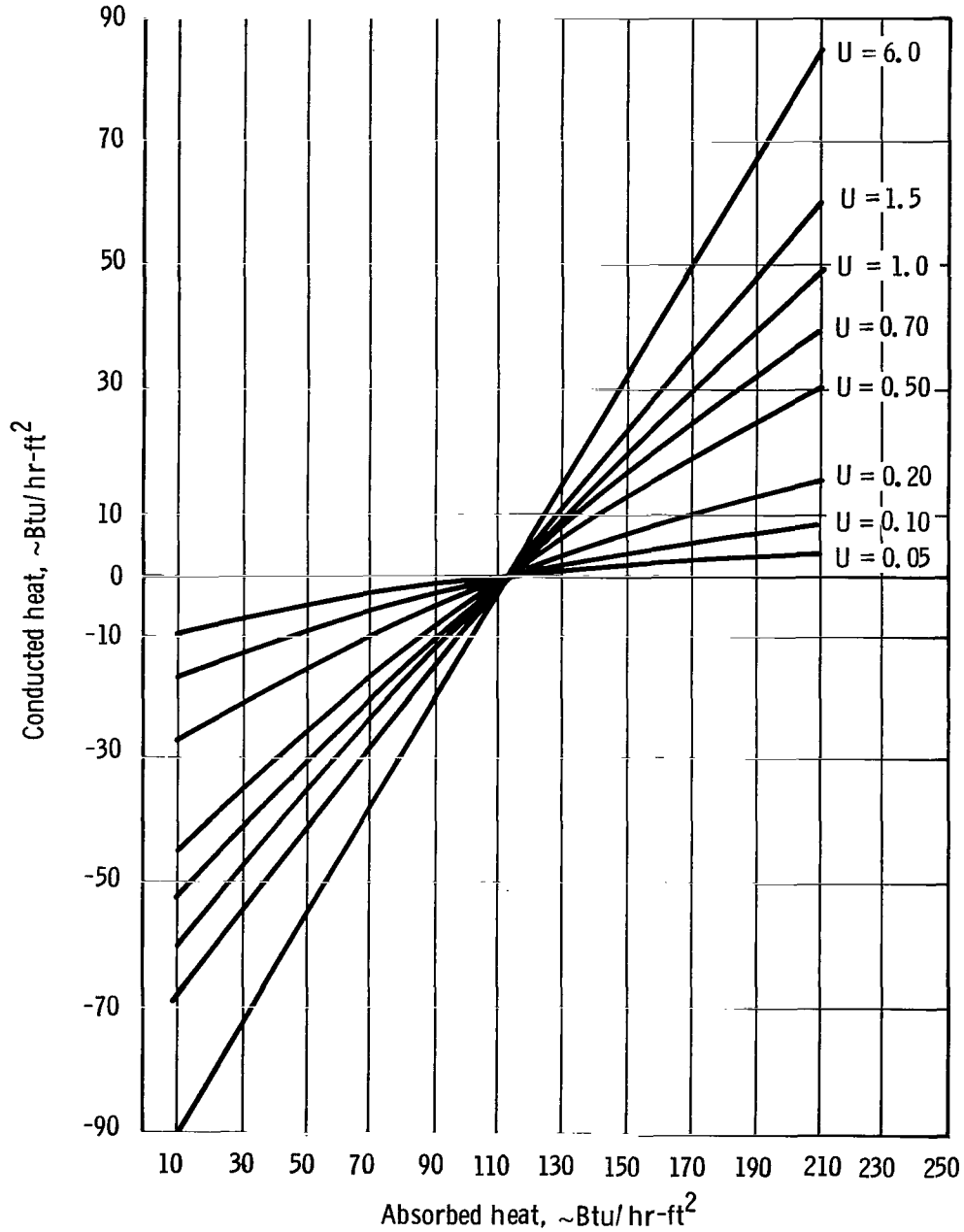

(p) U = 0.05 to 6.0, ϵ = 0.80.

Figure 14. - Continued.

NASA-S-67-5275

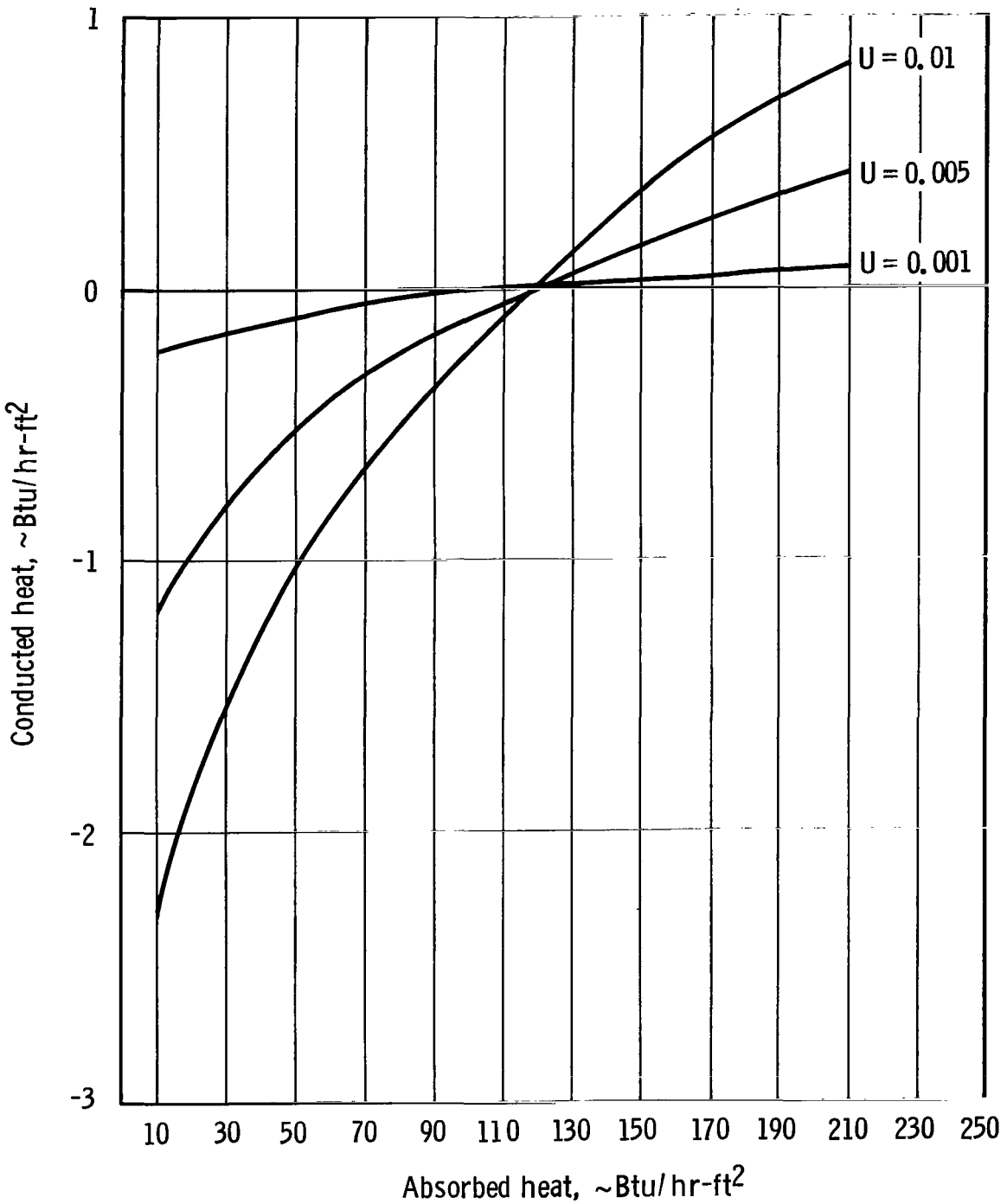

(q) U = 0.001 to 0.01, ϵ = 0.85.

Figure 14. - Continued.

NASA-S-67-5276

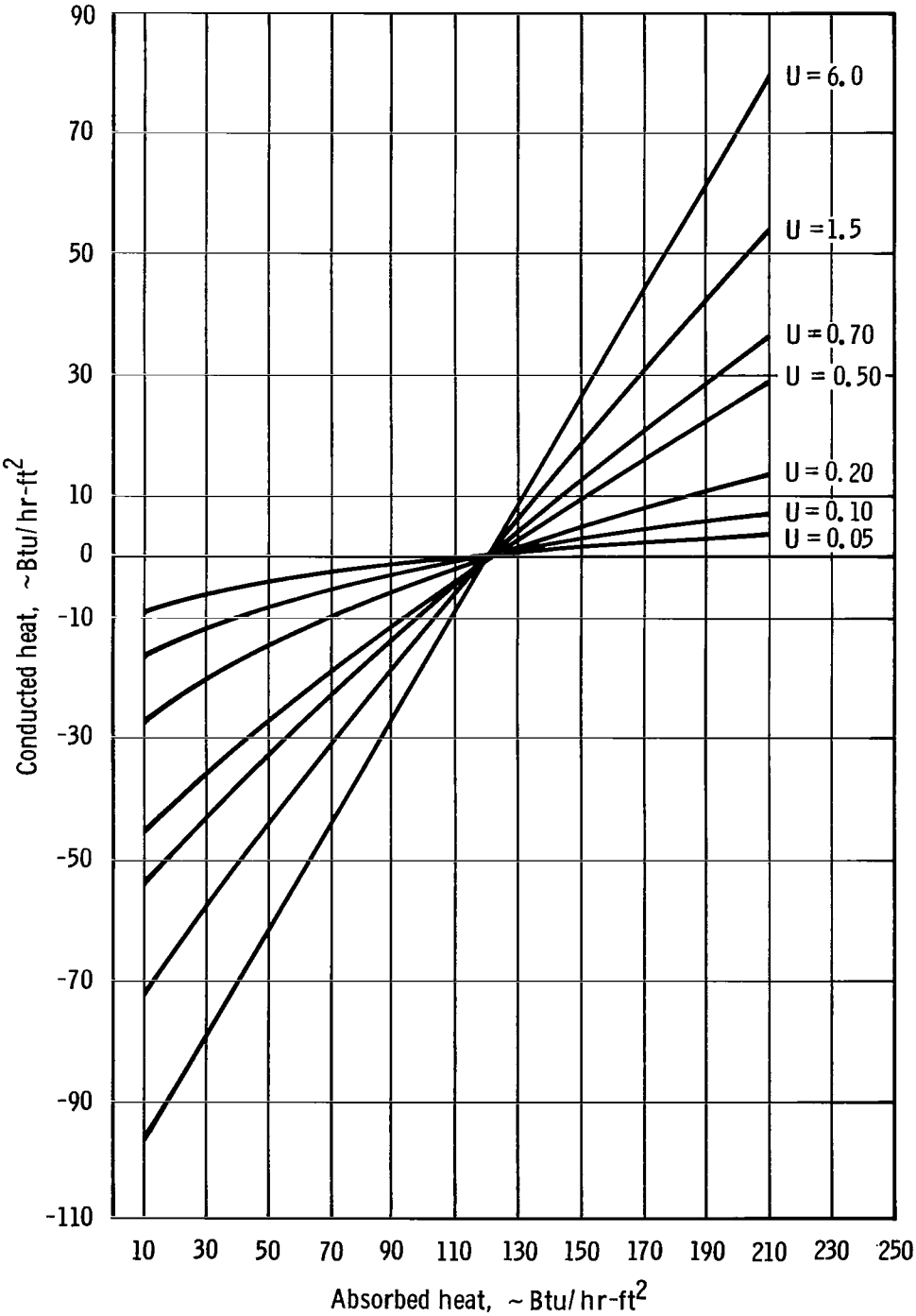

(r) U = 0.05 to 6.0, ϵ = 0.85.

Figure 14. - Continued.

NASA-S-67-5277

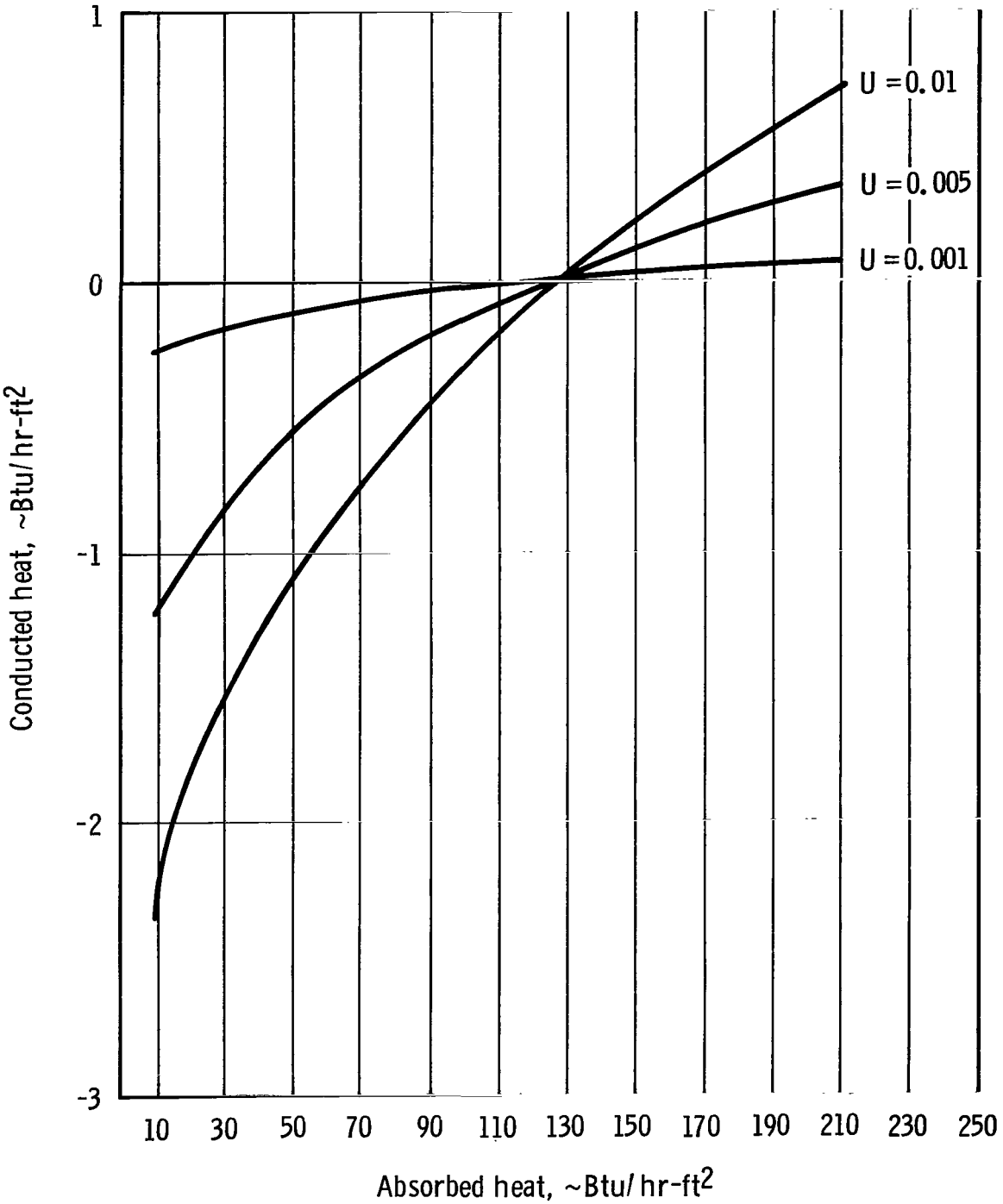

(s) U = 0.001 to 0.01, ϵ = 0.90.

Figure 14. - Continued.

NASA-S-67-5278

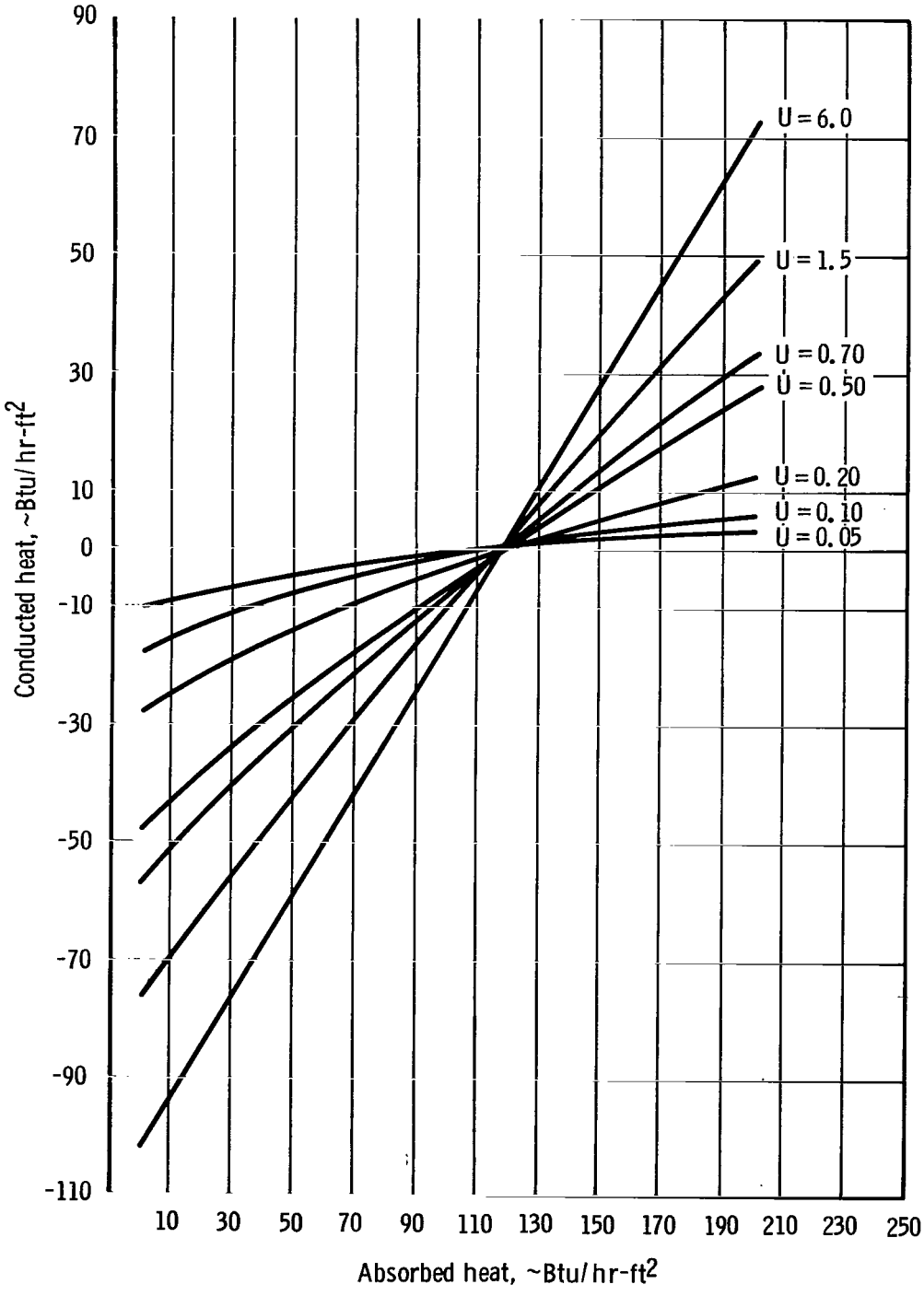

(t) U = 0.05 to 6.0, ϵ = 0.90.

Figure 14. - Continued.

NASA-S-67-5279

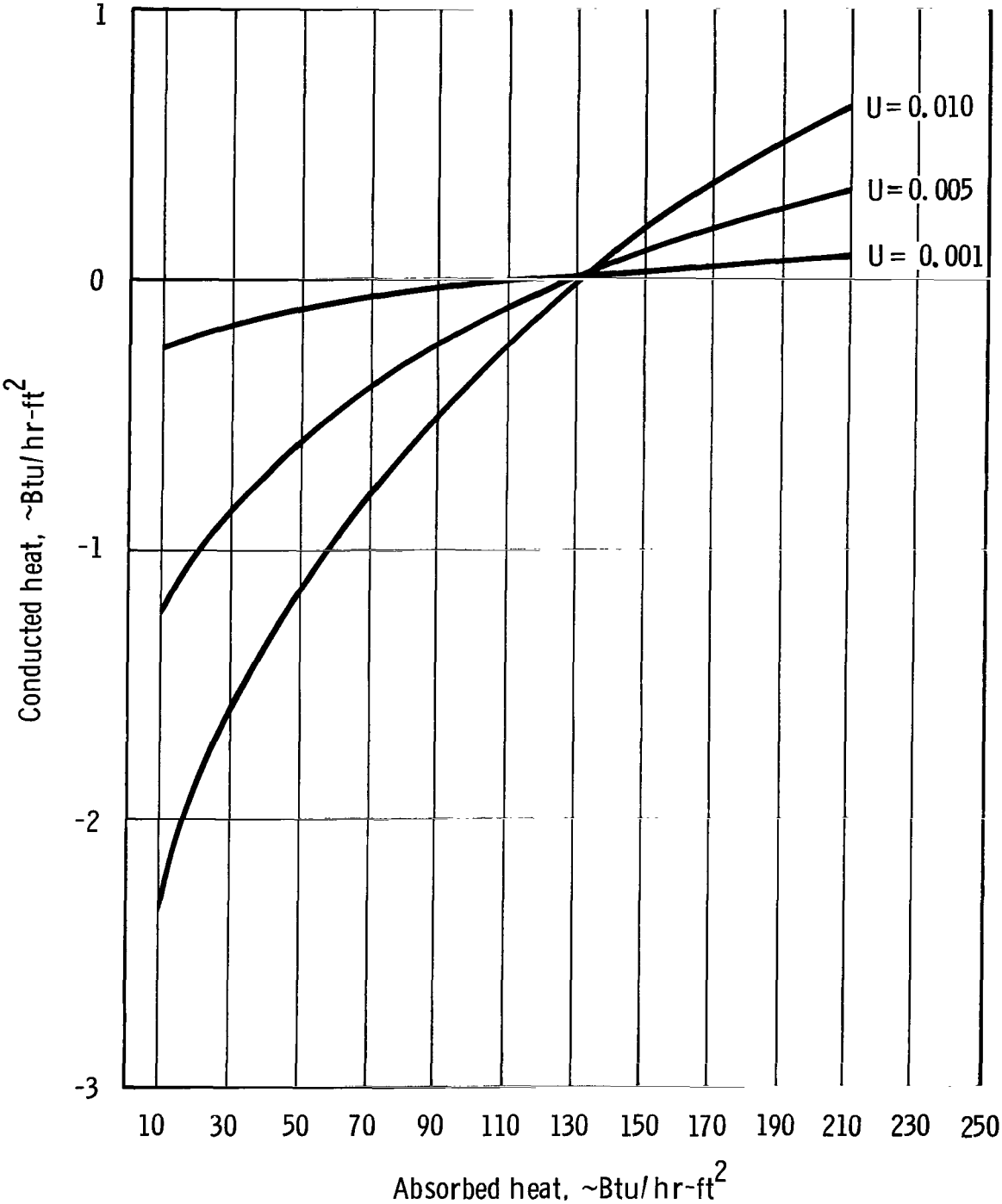

(u) U = 0.001 to 0.010, ϵ = 0.95.

Figure 14. - Continued.

NASA-S-67-5280

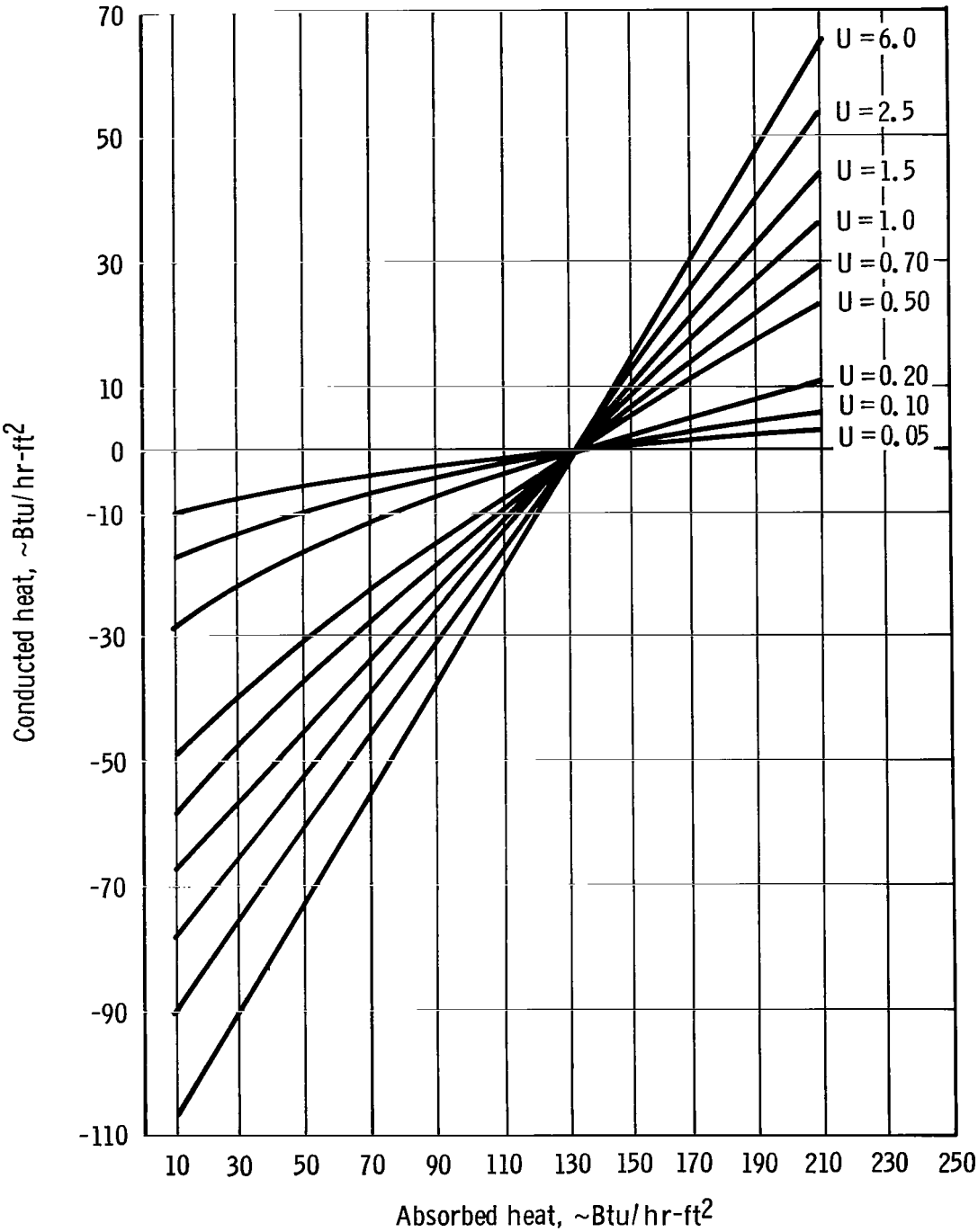

(v) U = 0.05 to 6.0, ϵ = 0.95.

Figure 14. - Concluded.

NASA-S-67-5281

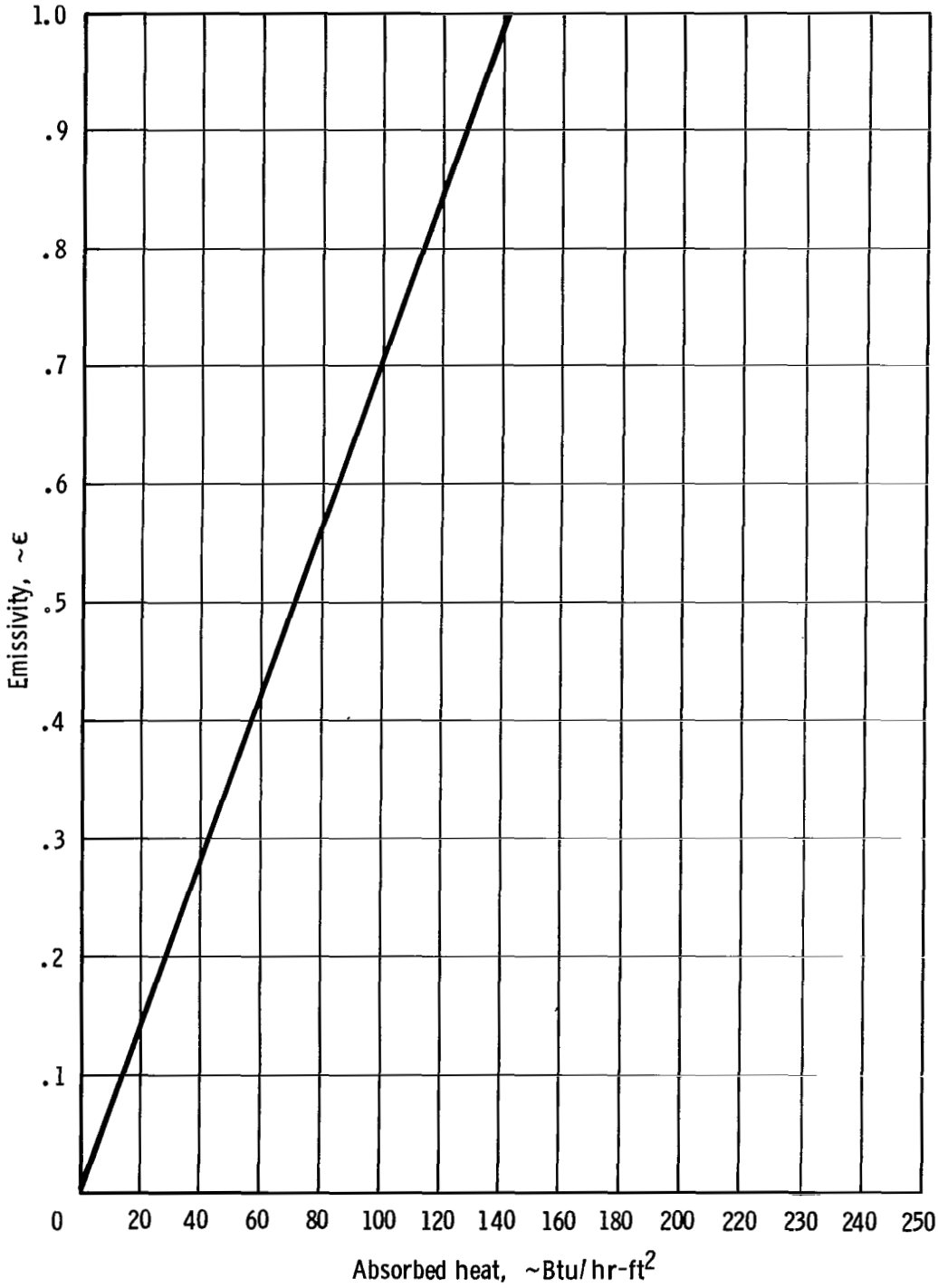

Figure 15. - Emissivity and absorbed heat causing zero heat conduction.

NASA-S-67-5238

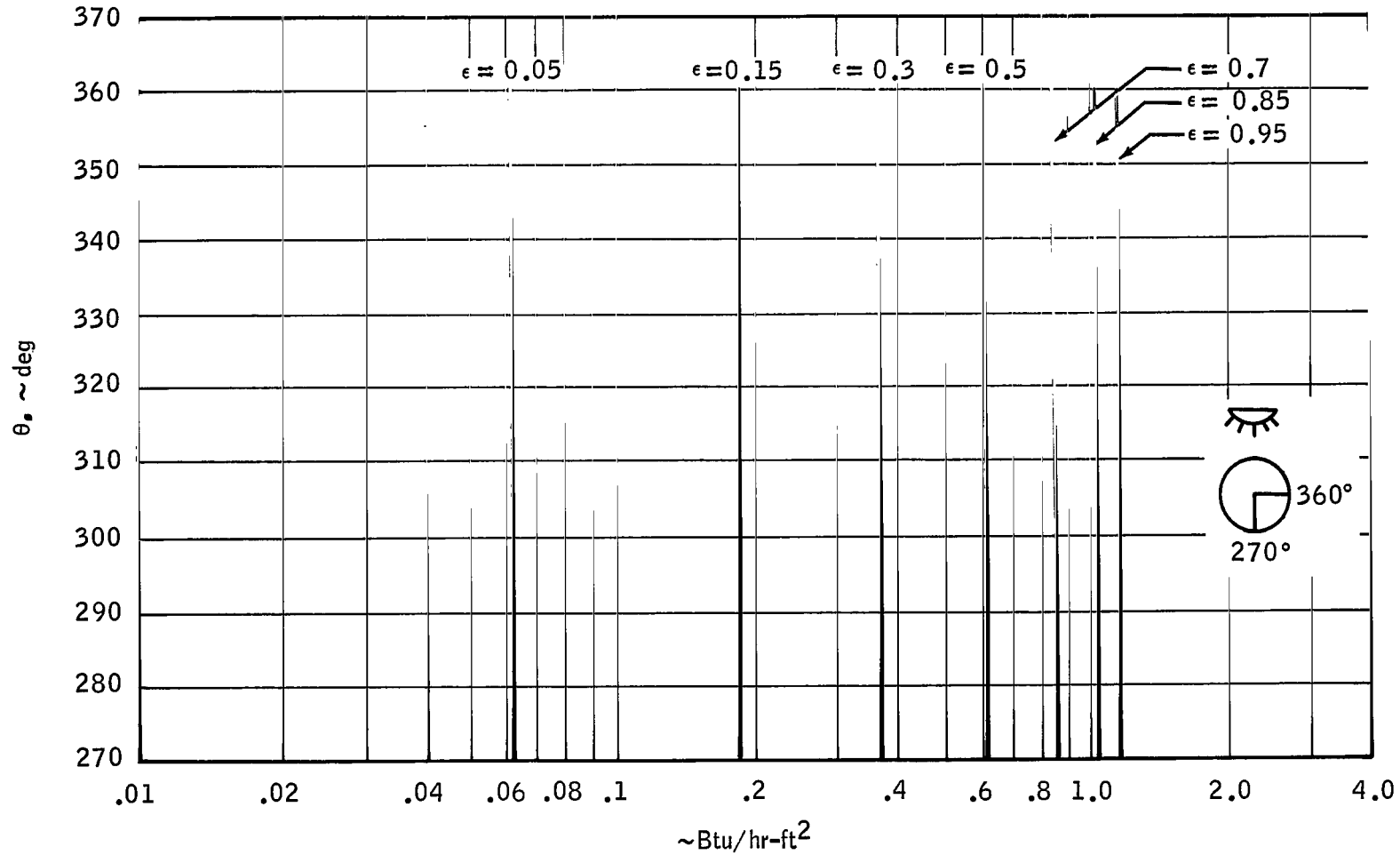

Figure 16. - Total heat absorbed per unit of surface area.

NASA-S-67-5239

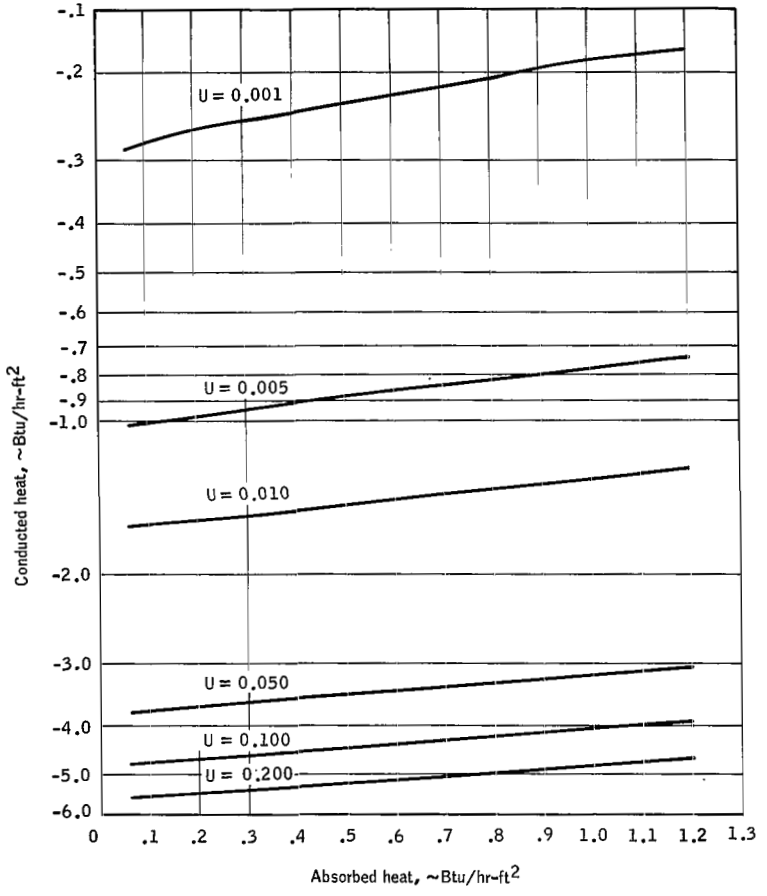

(a) U = 0.001 to 0.200, ϵ = 0.05.

NASA-S-67-5240

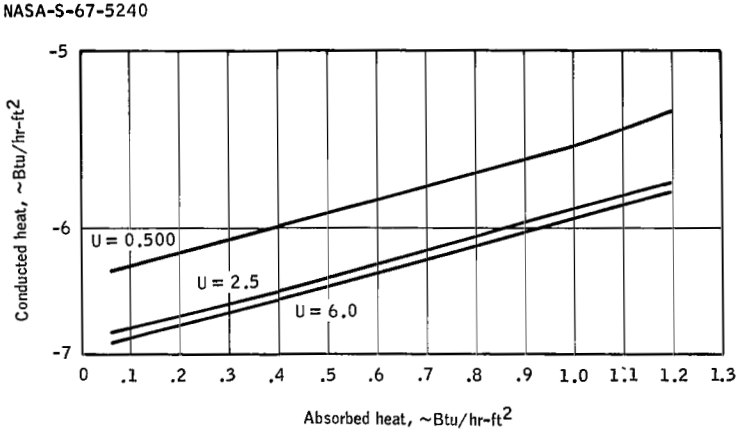

(b) U = 0.500 to 6.0, ϵ = 0.05.

Figure 17. - Plot of the conducted heat as a function of absorbed heat for the overall heat-transfer coefficient.

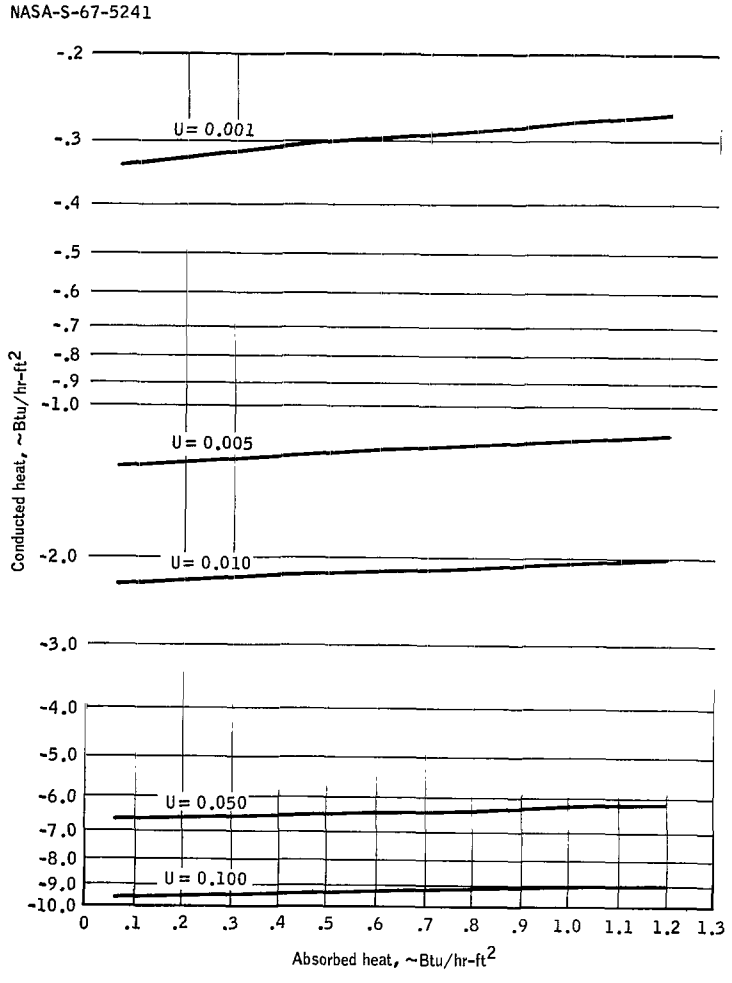

(c) U = 0.001 to 0.100, ϵ = 0.15.

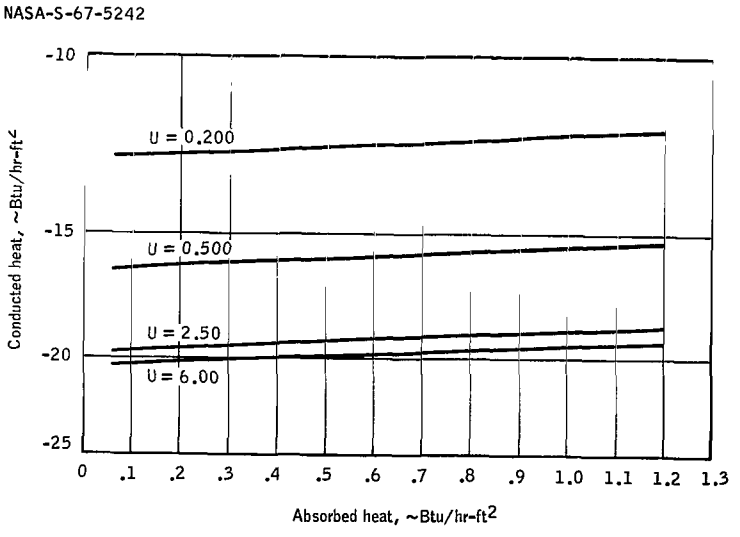

(d) U = 0.200 to 6.0, ϵ = 0.15.

Figure 17. - Continued.

NASA-S-67-5243

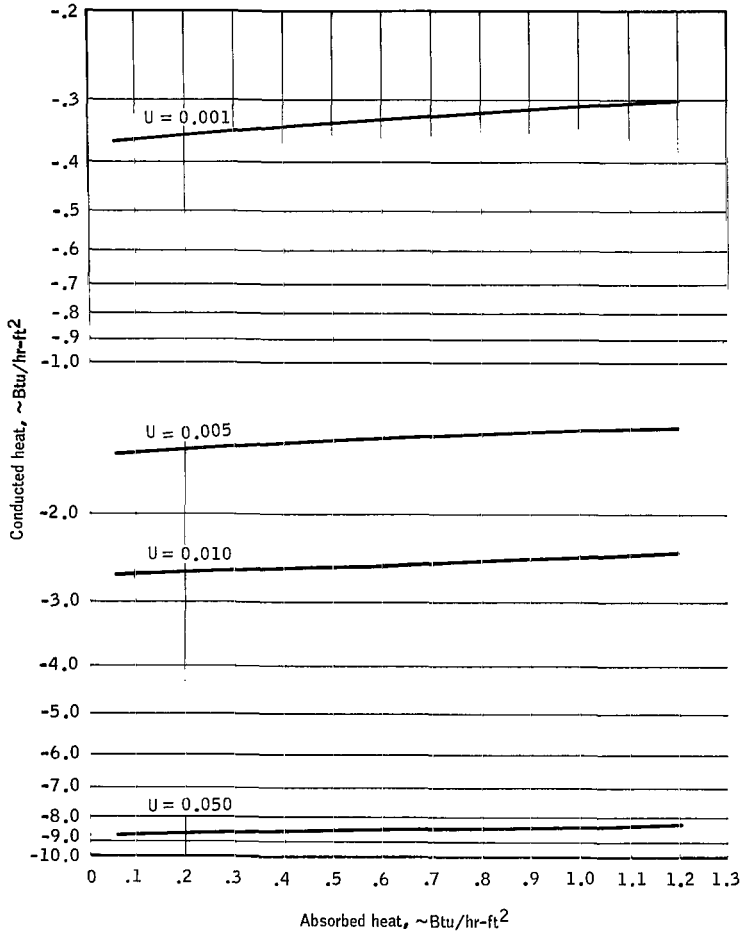

(e) U = 0.001 to 0.050, ϵ = 0.30.

NASA-S-67-5244

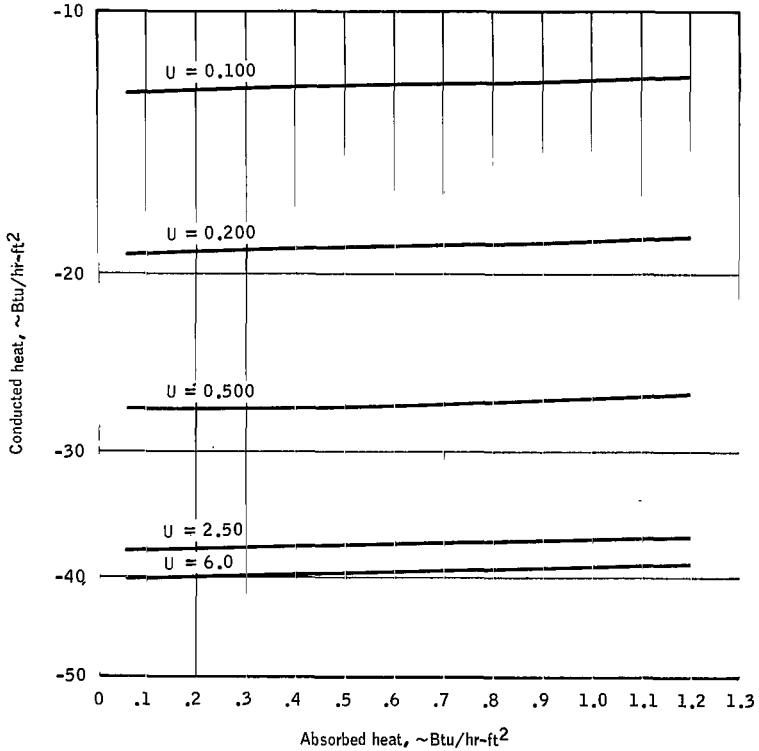

(f) U = 0.100 to 6.0, ϵ = 0.30.

Figure 17. - Continued.

NASA-S-67-5245

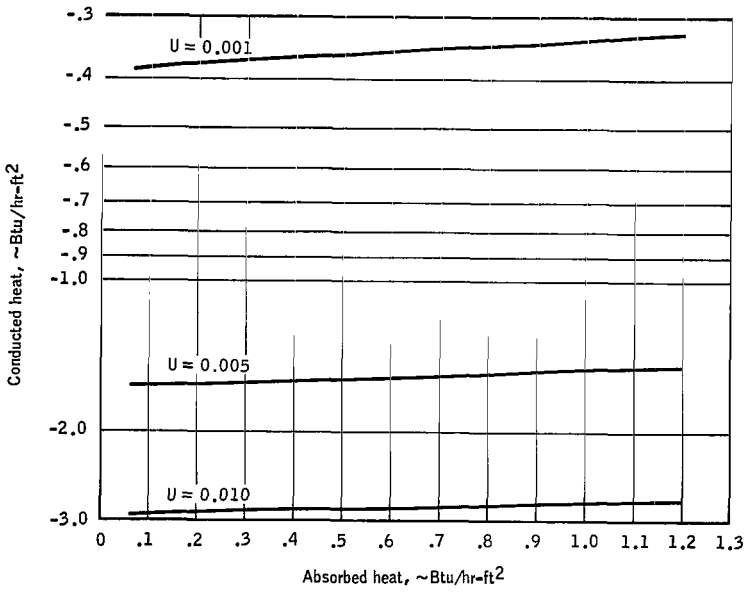

(g) U = 0.001 to 0.010, ϵ = 0.50.

NASA-S-67-5246

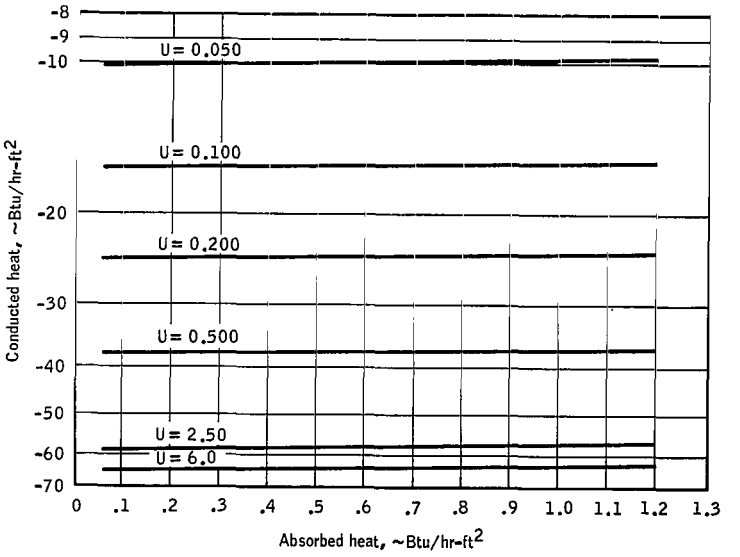

(h) U = 0.050 to 6.0, ϵ = 0.50.

(h) U = 0.050 to 6.0, ϵ = 0.50.

Figure 17. - Continued.

NASA-S-67-5247

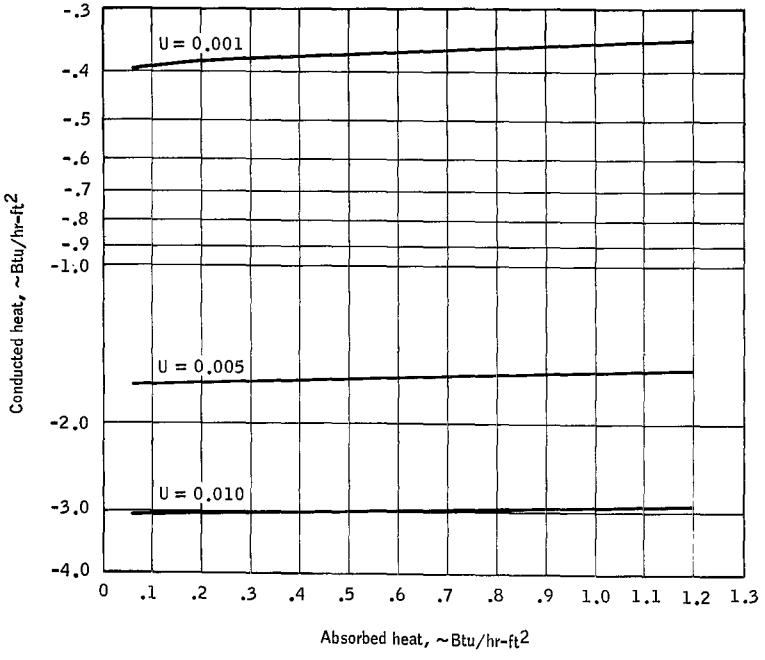

(i) U = 0.001 to 0.010, ϵ = 0.70.

NASA-S-67-5248

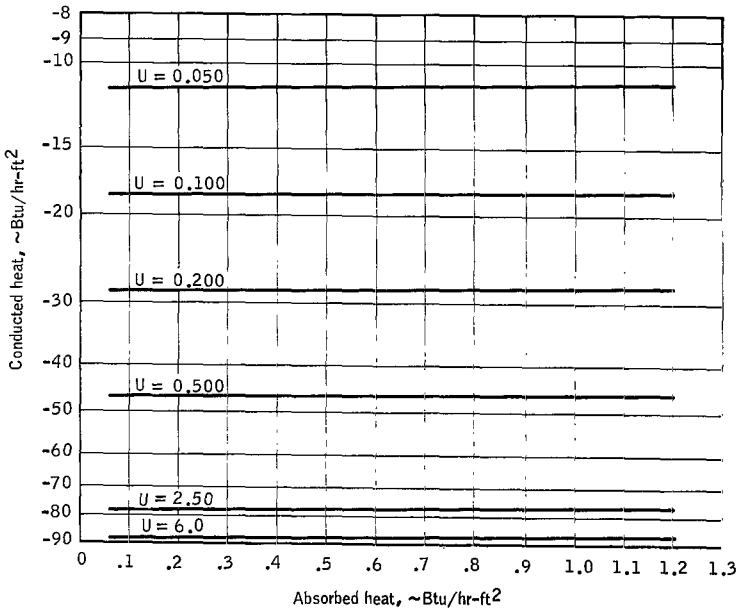

(j) U = 0.050 to 6.0, ϵ = 0.70.

Figure 17. - Continued.

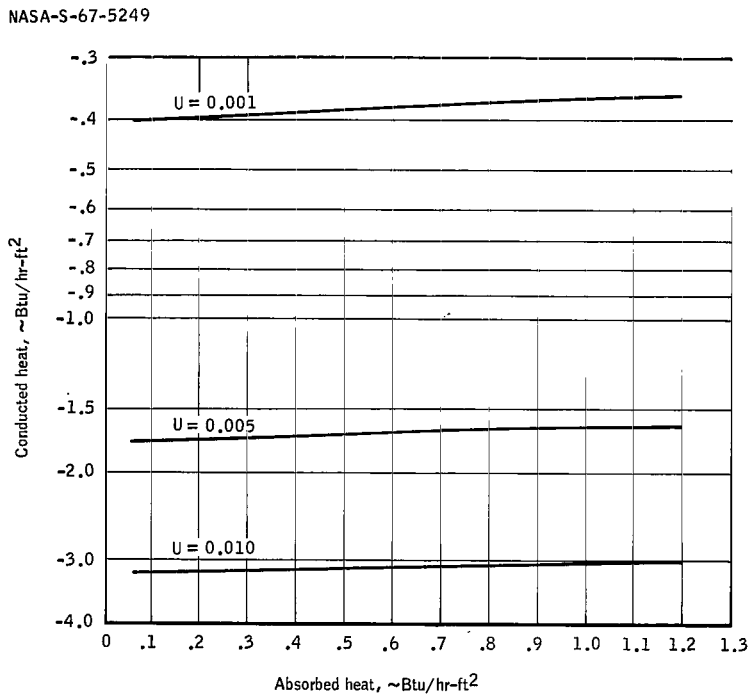

(k) U = 0.001 to 0.010, ϵ = 0.85.

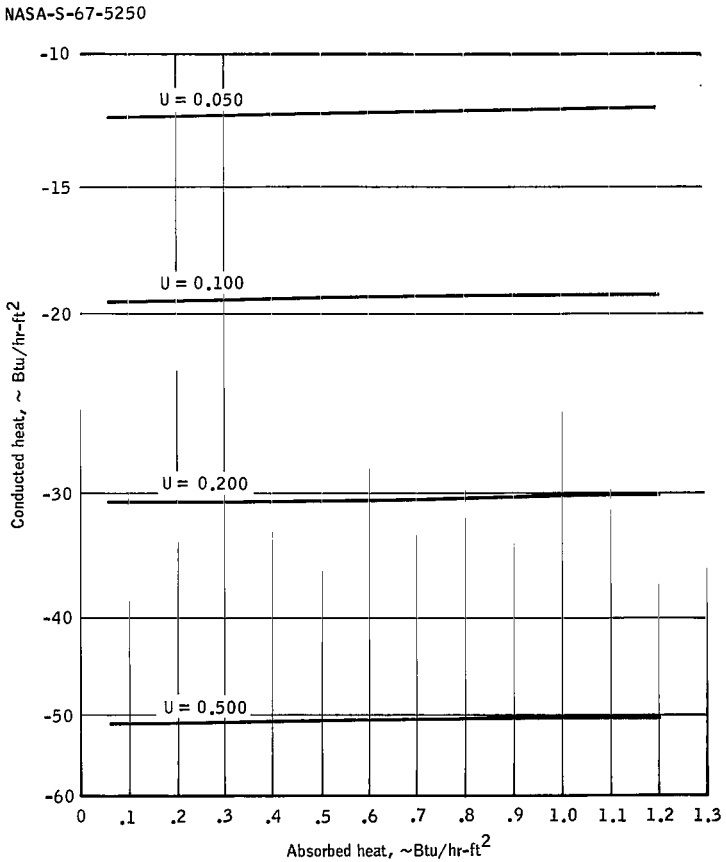

(l) U = 0.050 to 0.500, ϵ = 0.85.

Figure 17. - Continued.

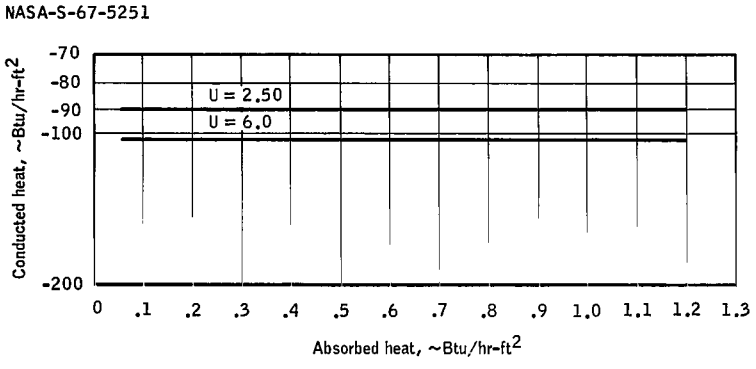

(m) U = 2.50 to 6.0, ϵ = 0.85.

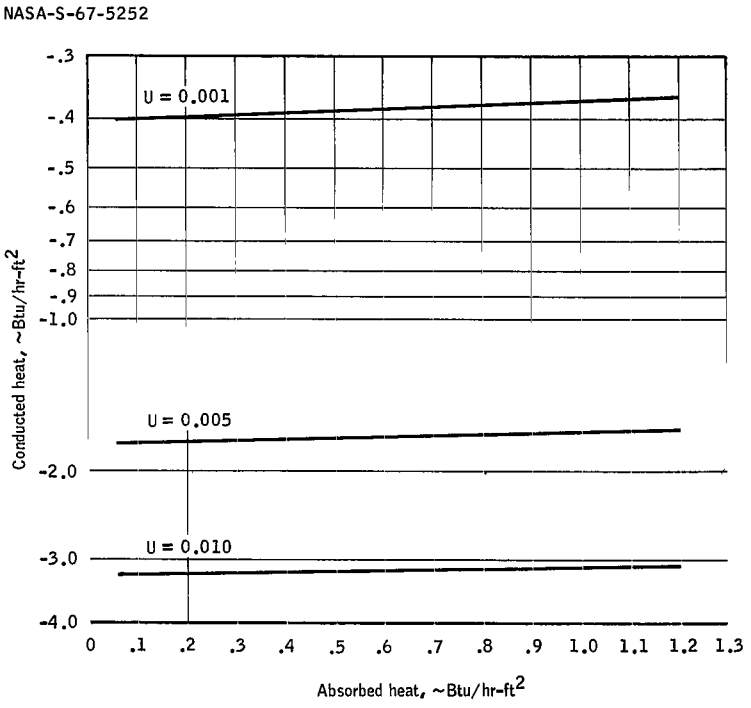

(n) U = 0.001 to 0.010, ϵ = 0.95.

Figure 17. - Continued.

NASA-S-67-5253

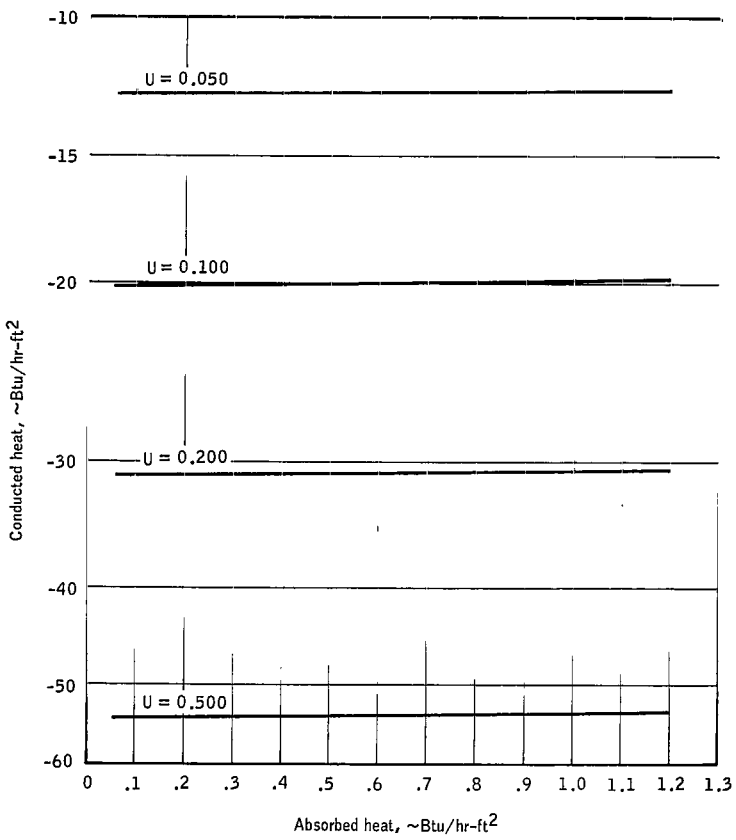

(o) U = 0.050 to 0.500, ϵ = 0.95.

NASA-S-67-5254

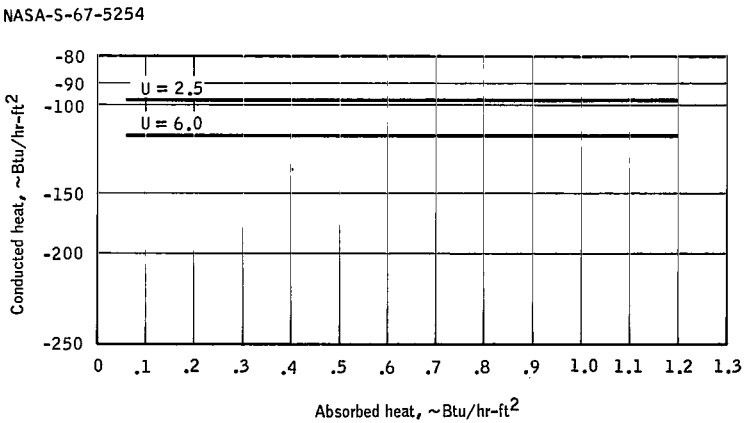

(p) U = 2.5 to 6.0, ϵ = 0.95.

Figure 17. - Concluded.

APPENDIX A

PROJECTED AREAS OF THE TORSO AND LEGS OF THE MULTICYLINDER MAN

In each instance, if the projected areas of the torso and legs of the multicylinder man are taken to be rectangles of height H sin ϕ, the problem is reduced to that of finding the projection of the exposed circumference normal to the direction of sight.

Ellipse

Figure A-1 illustrates the ellipse which is projected on the lunar plain by the torso (fig. 4). For a line-of-sight angle θ, C_p represents the projected length of the perimeter. From the geometry,

$$\left.\begin{aligned} x &= a\cos\phi & \qquad x &= R\cos\Psi \\ y &= b\sin\phi & \qquad y &= R\sin\Psi \end{aligned}\right\} \tag{A1}$$

for which

$$\frac{dy}{dx} = -\tan\theta = -\frac{b}{a}\frac{1}{\tan\phi} \tag{A2}$$

$$\frac{y}{x} = \frac{b}{a}\tan\phi = \tan\theta \tag{A3}$$

and

$$\tan\theta = \frac{b^2}{a^2}\frac{1}{\tan\Psi} \tag{A4}$$

The desired projection C_p is

$$C_p = 2R\cos\left(\frac{\pi}{2} - \theta - \Psi\right) = 2\sqrt{x^2 + y^2}\sin(\theta + \Psi) = 2a\cos\phi\sqrt{1 + \frac{b^2}{a^2}\tan^2\phi}\sin(\theta + \Psi) \tag{A5}$$

Further manipulation leads to

$$C_p = 2a\sqrt{1 - \left(\frac{a^2 - b^2}{a^2}\right)\cos^2\theta} \tag{A6}$$

Tangent Cylinders

Figure A-2 illustrates the top view of the legs. Radiation to cylinder X from quadrants 3 and 4 is desired. For a given line-of-sight angle θ, the projection C_p of the circumference of cylinder X, as viewed from quadrant 4, must be found. The tangent lines to the two cylinders define C_p. The distances a, b, and c are shown. The following relationships are evident

$$C_p = \frac{D}{2} + a \tag{A7}$$

$$a = b \cos \theta \tag{A8}$$

$$b = D - c \tag{A9}$$

and

$$c = \frac{\frac{D}{2}}{\cos \theta} \tag{A10}$$

Substitution leads to the final result

$$C_p = D \cos \theta \tag{A11}$$

NASA-S-67-5255

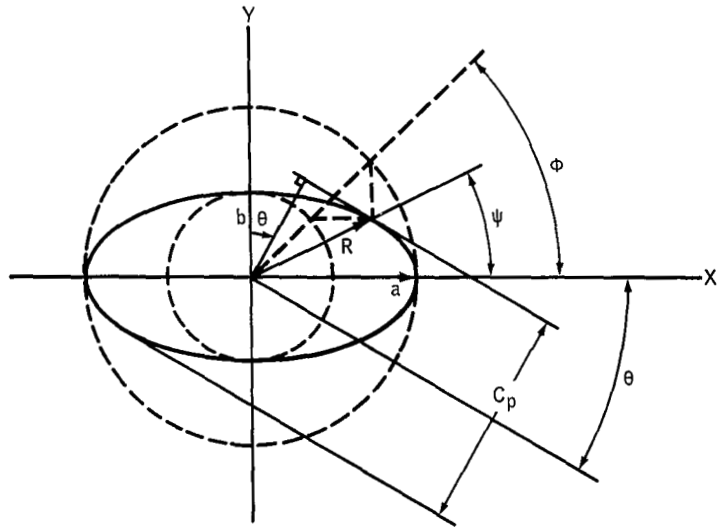

Figure A-1. - Ellipse.

NASA-S-67-5256

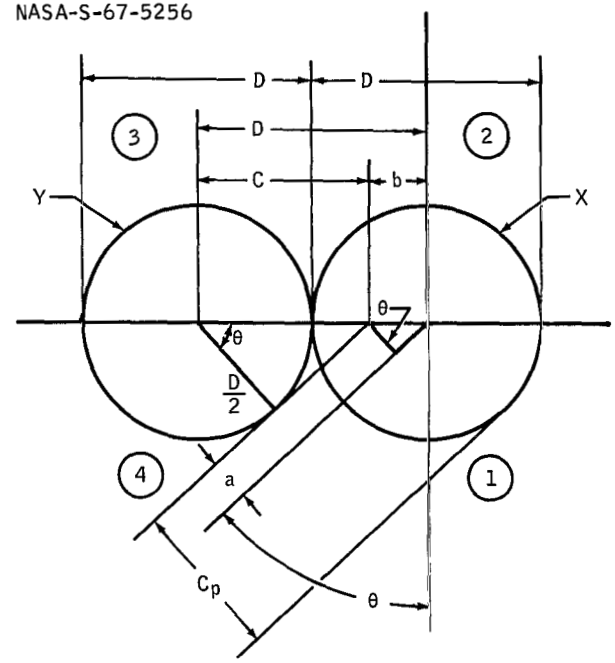

Figure A-2. - Top view of legs on the lunar plain.

APPENDIX B

PROJECTED AREA OF THE HEAD OF THE HEMISPHERE-CYLINDER MAN

Figure B-1 shows the hemisphere viewed from a point on a plane. The projected area A_p normal to the line of sight is seen to be the difference between the area of a semicircle (radius = a) and a semiellipse (semimajor diameter = a, semiminor diameter = 2 cos ϕ). Thus

$$A_p = \frac{\pi a^2}{2} - 0.5\,\pi a(a \cos \phi) = \frac{\pi a^2}{2}(1 - \cos \phi) \qquad \text{(B1)}$$

NASA-S-67-5257

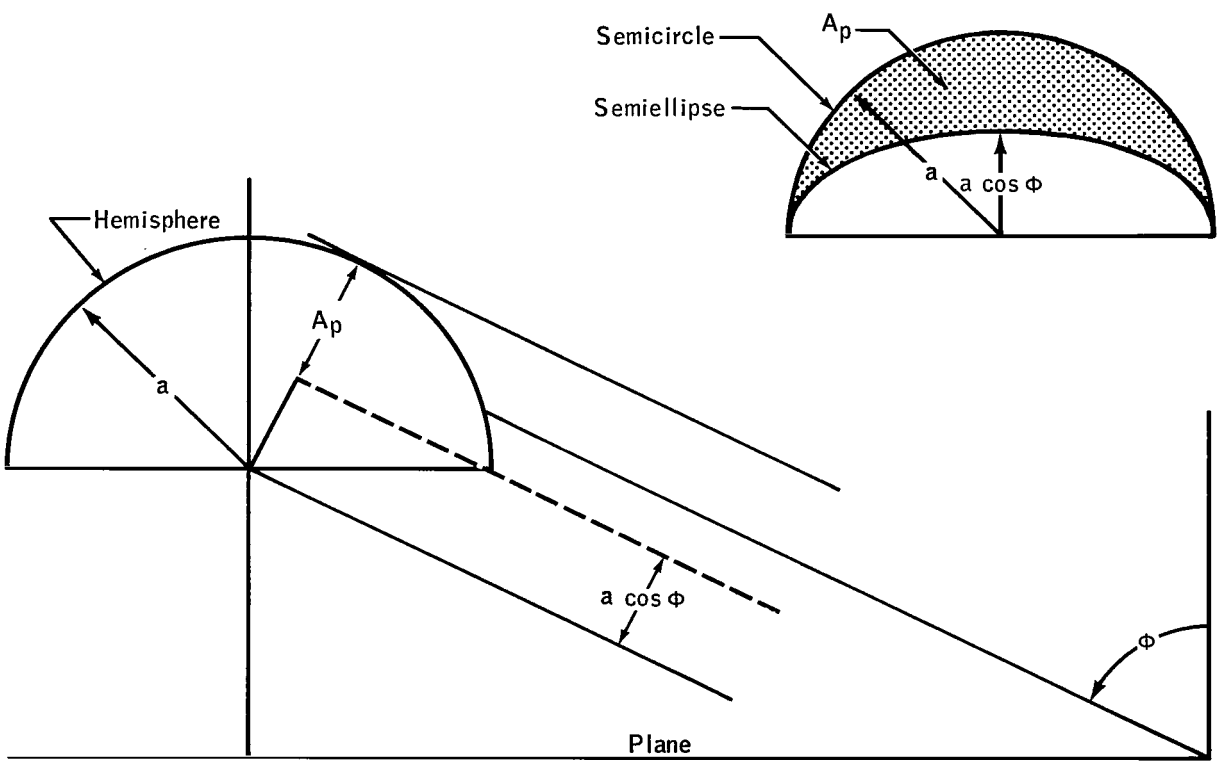

Figure B-1. - Hemisphere viewed by parallel rays from a point on a plane.

APPENDIX C

TOTAL HEAT ABSORPTION PER UNIT AREA OF THE HEMISPHERE-CYLINDER MAN

Neglecting the multiple reflections between the moon's surface and the man (fig. C-1), the following heat balance may be written.

$$q_{abs} = q_s + q_{em} + q_{am} \tag{C1}$$

By use of the definitions

$$q_s = \alpha_s \left(G_s A_{ps}\right) \tag{C2}$$

$$q_{em} = \epsilon \left(eFA_t\right) \tag{C3}$$

and

$$q_{am} = \alpha_s a F_s G_s F A_t \tag{C4}$$

In equation (C3) the basic reciprocity property of the shape factor (ref. 1) has been used. Assuming that equilibrium exists between the sun and the moon's surface,

$$e = G_n(1 - a) = F_s G_s(1 - a) \tag{C5}$$

Thus

$$q_{abs} = \alpha_s G_s A_{p_s} + \epsilon G_s F_s (1 - a) F A_t + \alpha_s a F_s G_s F A_t \tag{C6}$$

$$\frac{q_{abs}}{A_t} = G_s \left\{ \alpha_s F_m + \left[\epsilon (1 - a) + \alpha_s a \right] F F_s \right\} \tag{C7}$$

Special cases of this expression may be obtained for specific assumed geometries of man.

For the hemisphere-cylinder combination, the projected area A_{p_s} may be taken as the sum of a rectangle and the projected area of the hemisphere. If the cylinder is of height H and diameter D, then the rectangle has an area of HD cos θ. The projected area of the hemisphere is the sum of the area of a semicircle of diameter D, $0.5\,\pi(D/2)^2$, and the area of a semiellipse of major diameter D and minor diameter D sin θ. This area is, then, $0.5\,\pi(D/2)^2 \sin\theta$. Thus

$$A_{p_s} = HD\cos\theta + 0.125\,\pi D^2\,(1 + \sin\theta) \tag{C8}$$

Since

$$A_t = \pi DH + \frac{\pi D^2}{2} \tag{C9}$$

then

$$F_m = \frac{A_{p_s}}{A_t} \tag{C10}$$

is

$$F_m = \frac{\frac{1}{\pi}\cos\theta + 0.125\,\frac{D}{H}\,(1 + \sin\theta)}{1 + 0.5\,\frac{D}{H}} \tag{C11}$$

If the expression for F_m and the relationships of F_s in figure 9 are introduced into the equation for q_{abs}/A_t, then an expression for the heat absorbed by a hemisphere-cylinder man is obtained as a function of only the geometrical parameters H and D, the surface properties ϵ and α_s, the moon's albedo a, and the angular position θ. Figure 11 was computed by this means.

The point of maximum heat absorption may be found by examining the derivative

$$\frac{d}{d\theta}\left(\frac{q_{abs}}{A_t G_s}\right) = \alpha_s \frac{dF_m}{d\theta} + \left[\epsilon(1 - a) + \alpha_s a\right] F \frac{dF_s}{d\theta} \tag{C12}$$

For the hemisphere-cylinder man, the expression for F_m may be used so that the point of maximum heat absorption is given by

$$\frac{\alpha_s}{1 + 0.5\frac{D}{H}}\left(-\frac{1}{\pi}\sin\theta + 0.125\frac{D}{H}\cos\theta\right) + \left[\epsilon(1 - a) + \alpha_s a\right] F \frac{dF_s}{d\theta} = 0 \tag{C13}$$

Treating the two ranges of F_s separately

$$F_s = \sin\theta \tag{C14}$$

where $28.26° \leq \theta \leq 90°$, and

$$F_s = 0.039 + 0.8808\theta \tag{C15}$$

where $0° \leq \theta \leq 28.26°$. Thus, the maximum heat-absorption position is given by

$$\theta_{q_{max}} = \tan^{-1}\left(\pi\left\{0.125\frac{D}{H} + F\left(1 + 0.5\frac{D}{H}\right)\left[\frac{\epsilon}{\alpha_s}(1 - a) + a\right]\right\}\right) \tag{C16}$$

where $28.26° \leq \theta \leq 90°$ and $\theta_{q_{max}}$ is the root of

$$\frac{1}{\pi}\sin\theta_{q_{max}} - 0.125\frac{D}{H}\cos\theta_{q_{max}} = F\left(1 + 0.5\frac{D}{H}\right)\left[\frac{\epsilon}{\alpha_s}(1 - a) + a\right]0.8808 \tag{C17}$$

where $0° \leq \theta \leq 28.26°$. These expressions were used with D/H = 1.52/5.0 and a = 0.07 to obtain figures 12 and 13.

NASA-S-67-5258

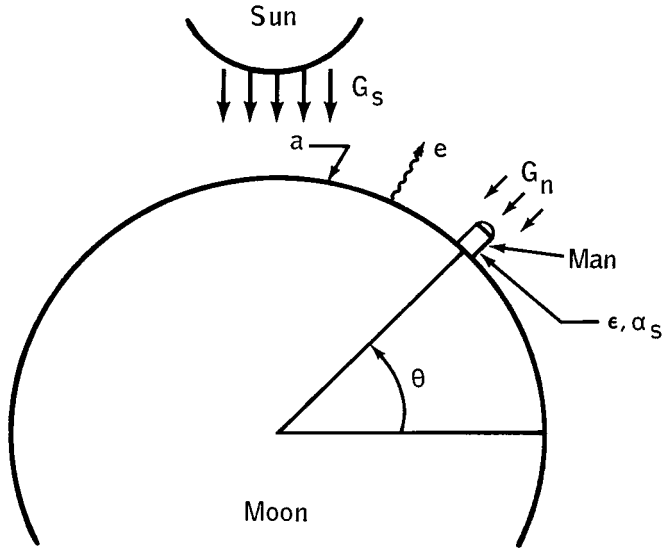

Figure C-1. - Hemisphere-cylinder man's total heat absorption per unit area.

REFERENCES

1. Chapman, Alan J.: Heat Transfer. Second ed. Macmillan Co. (New York), 1967.

2. Clarke, R. C.: An Approximation Procedure for Determining Configuration Factors in Radiative Heat Transfer Problems. M. S. Thesis, Rice University (Houston, Texas), May 1964.

3. Burris, W. L.; and Lin, S. H.: Study of the Thermal Processes for Man in Space. NASA CR-216, April 1965.

4. Kopal, Z., ed.: Physics and Astronomy of the Moon. Academic Press, 1962.

5. Arvensen, John C.; and Hamaker, Frank M.: Effectiveness of Radiation Shields for Thermal Control of Vehicles on the Sunlit Side of the Moon. NASA TN D-2130, 1964.

NASA-Langley, 1967 —— 30 S-100

"The aeronautical and space activities of the United States shall be conducted so as to contribute . . . to the expansion of human knowledge of phenomena in the atmosphere and space. The Administration shall provide for the widest practicable and appropriate dissemination of information concerning its activities and the results thereof."

—NATIONAL AERONAUTICS AND SPACE ACT OF 1958

NASA SCIENTIFIC AND TECHNICAL PUBLICATIONS

TECHNICAL REPORTS: Scientific and technical information considered important, complete, and a lasting contribution to existing knowledge.

TECHNICAL NOTES: Information less broad in scope but nevertheless of importance as a contribution to existing knowledge.

TECHNICAL MEMORANDUMS: Information receiving limited distribution because of preliminary data, security classification, or other reasons.

CONTRACTOR REPORTS: Scientific and technical information generated under a NASA contract or grant and considered an important contribution to existing knowledge.

TECHNICAL TRANSLATIONS: Information published in a foreign language considered to merit NASA distribution in English.

SPECIAL PUBLICATIONS: Information derived from or of value to NASA activities. Publications include conference proceedings, monographs, data compilations, handbooks, sourcebooks, and special bibliographies.

TECHNOLOGY UTILIZATION PUBLICATIONS: Information on technology used by NASA that may be of particular interest in commercial and other non-aerospace applications. Publications include Tech Briefs, Technology Utilization Reports and Notes, and Technology Surveys.

Details on the availability of these publications may be obtained from:

SCIENTIFIC AND TECHNICAL INFORMATION DIVISION

NATIONAL AERONAUTICS AND SPACE ADMINISTRATION

Washington, D.C. 20546